Dynamical chaos in magnetic systems

K. N. Alekseev, G. P. Berman, V. I. Tsifrinovich, and A. M. Frishman

L. V. Kirenski Institute of Physics, Russian Academy of Sciences, Krasnoyarsk
(Submitted 27 September 1991; resubmitted after revision 26 February 1992)
Usp. Fiz. Nauk **162**, 81–118 (July 1992)

The theoretical and experimental studies on the transition to dynamical chaos in magnetic systems are reviewed. Both dissipative and Hamiltonian systems are discussed, with their fundamental scenarios of the transition to chaos. We discuss the models and characteristics of chaotic oscillations in magnetic materials upon parametric excitation of spin waves, in NMR masers, in the dynamics of spin chains, in the motion of a spin in an external alternating magnetic field, and in nonlinear NMR with dynamic shift of the precession frequency. An analysis of the problems of quantum chaos in spin systems is presented.

"Chaos is the score upon which reality is written"
(Henry Miller, "Tropic of Cancer")

1. INTRODUCTION

In recent years the ideas, concepts, and methods of the theory of nonlinear processes have substantially enriched many fields of physics, from elementary-particle physics to biophysics.[1,2] At present an independent field in nonlinear physics is the study of chaos in various dynamical systems.[3–9] Chaos in this case is not associated with the presence of any random parameters and forces, but is due to the unstable character of the behavior of trajectories in phase space.[1)]

The aim of this review is to introduce the rapidly developing study of the phenomenon of chaos in magnetic (spin) systems. The variety of mechanisms of creating nonlinearity, the simple methods of controlling various parameters, and not last, the considerable experience accumulated in studying nonlinear phenomena—all this renders the physics of magnetic phenomena a natural field for studying such a general phenomenon as dynamical chaos. Now new characteristics have been required to describe the dynamics of magnetic systems—such as the fractal dimension, the Lyapunov indices, the Kolmogorov entropy, and nonlinear resonances and their overlap, etc. The use of the methods of chaos theory has enabled finding a new approach to a number of old problems of the physics of magnetic phenomena. Thus, for example, it has turned out that the well known Suhl instabilities are elementary bifurcations on the pathway to the few-mode chaos of spin waves with formation of a strange attractor.

A common modern tendency in the study of nonlinear dynamics in physical systems is to separate the study of chaos in each individual field of physics into an independent field (e.g., optical chaos[11]). Apparently the same happens in the physics of magnetic phenomena, where the study of "magnetic chaos" or "magnetic turbulence" is being shaped in essence into an independent field of magnetism.

Chaos in magnetic systems can be observed both in a steady-state regime (dissipative chaos, strange attractor), and in a transitional regime (dissipation-free or Hamiltonian chaos). Such a classification of magnetic chaos into Hamiltonian and dissipative types is, on the one hand, rather natural and generally accepted in the study of other physical systems, and on the other hand, it is necessary, since chaos in Hamiltonian and dissipative systems has a number of substantially different features. This review will discuss examples of both dissipative and Hamiltonian chaos in magnetic systems. We have focused attention on systems where magnetic chaos has been studied most fully: nonlinear interactions of spin waves in the case of parametric pumping, spin chains, and a spin in an external alternating magnetic field, NMR masers, and NMR with a dynamic shift of the precession frequency of the magnetization. We also discuss the phenomenon of quantum chaos in spin systems. The order of arrangement of the material in the review reflects the degree of study of the discussed systems.

Before we proceed to present the characteristic features of the transition from regular behavior to chaos in magnetic systems, we shall take up briefly the main features of chaos and the criteria for its onset in very simple Hamiltonian and dissipative dynamical systems.

2. OVERALL CONCEPTS ON THE TRANSITION OF CHAOS IN DYNAMICAL SYSTEMS

At present the fundamental conditions for transition to chaos in simple Hamiltonian and dissipative systems are rather well known.[1,4–9] An important circumstance is that a large number of degrees of freedom is not required for the onset of chaos—one degree of freedom suffices when interacting with an external periodic field (1.5 degrees of freedom). Conversely, an extensive class exists of the so-called completely integrable systems,[12,13] including an infinite number of degrees of freedom, in which a transition to chaos is not realized under any conditions.

As the fundamental characteristics of dynamical chaos we present the following: local instability of trajectories in phase space;[2)] fast (especially in the initial stage) decay of the phase correlation functions, a consequence of which is diffusion of Brownian type in the slow variable; and a continuous frequency spectrum of the dynamical variables.

Now let us study some very simple dynamical systems with chaotic dynamics: the Chirikov mapping (or standard mapping),[3,4] which arises in studying the dissipation-free motion of a plane rotator interacting with a periodic sequence of brief impulses;[3)] the Zaslavskiĭ mapping,[5] which takes account of the effects of dissipation in the previous problem; and the logistic mapping—one of the simplest examples of a dynamical system with chaos, the transition to

 0038-5670/92/070572-19$03.00

which is analogous in many ways to the transition to chaos in magnetic systems with a small number of degrees of freedom.

2.1. Chaos in Hamiltonian systems. Stochasticity parameter. Chirikov criterion of overlap of nonlinear resonances

In the theory of dynamical chaos in Hamiltonian classical systems useful concepts characterizing the transition to chaos are the stochasticity parameter and the Chirikov parameter of overlap of nonlinear resonances.[3,4] Let us introduce these concepts here using a very simple example of a nonlinear system—a plane rotator interacting with an external field in the form of an infinite periodic sequence of δ-function pulses. The Hamiltonian of the system has the form

$$H(J,\theta,t)=\frac{G}{2}J^2+\varepsilon T\cos\theta\cdot\delta_T(t), \tag{2.1}$$

$$\delta_T(t)=\sum_{n=-\infty}^{+\infty}\delta(t-nT)=\frac{1}{T}\sum_{n=-\infty}^{+\infty}\exp(in\nu t)\quad(\nu=2\pi/T).$$

Here G is the reciprocal moment of inertia of the rotator, ε is the amplitude of the external field, J and θ are the action and the phase of the rotator, and T is the period of the sequence of pulses. The equations of motion for J and θ have the form

$$\dot J=-\frac{\partial H}{\partial\theta}=\varepsilon T\sin\theta\cdot\delta_T(t)=\frac{\varepsilon}{T}\sum_{n=-\infty}^{+\infty}\cos(\theta-n\nu t), \tag{2.2}$$

$$\dot\theta=\frac{\partial H}{\partial J}=GJ\equiv\omega(J).$$

Integration of the equations of motion (2.2) over the time interval $t_{n-1}-0\div t_n-0(t_n\equiv nT)$ leads to the Chirikov mapping (standard mapping)[3,4]

$$\begin{aligned}I_n&=I_{n-1}+K\sin\theta_{n-1},\\ \theta_n&=\theta_{n-1}+I_n(\mathrm{mod}\ 2\pi),\end{aligned} \tag{2.3}$$

Here we have $I_n=I(t_n-0)=GTJ_n$, $\theta_n\equiv\theta(t_n-0)$, $K\equiv\varepsilon GT$. The discrete mapping (2.3) conserves the area in phase space: $|\partial(I_n,\theta_n)/\partial(I_{n-1},\theta_{n-1})|=1$. According to (2.3) each initial point (I_0,θ_0) corresponds to a certain phase trajectory that depends on the single parameter K, which is called the stochasticity parameter. Figure 1 shows the form of the phase space for different values of the stochasticity parameter K. We should immediately note a very important circumstance—even in the very simple case of the system of (2.1) with 1.5 degrees of freedom, the phase space, as we see from Fig. 1, is rather complicated (the points in Fig. 1b correspond to the single chaotic trajectory!), and it can be analyzed in detail only by using a computer. Thus at present the theoretical analysis of dynamical chaos, even in systems with a small number of degrees of freedom, can be conducted only within the framework of semiqualitative methods with subsequent introduction of numerical experiment. Below we shall examine in greater detail one of these methods based on the concept of interacting nonlinear resonances.

As we see from Fig. 1a, for sufficiently small K the phase space (I,θ) mainly contains two types of trajectories: 1) closed, corresponding to oscillatory motions in the vicinity of resonances; 2) open, corresponding to rotational motions. The closed and open trajectories are separated by separatrix layers, which contain stochastic trajectories. However, when $K\ll 1$ the dimensions of these layers are exponentially small with respect to action.[4] Analysis of the mapping of (2.3) shows that, when $K<K_c\approx 1$, global chaos is absent in the system of (2.1). That is, the chaotic phase trajectories lie in regions of phase space bounded in terms of action.

Let us determine the dimensions in terms of action δI_n of the regions of the primary resonances, whose centers J_n^0 are found from the equation: $\dot\theta=\omega(J^0)=n\nu$. Hence we obtain the following expression for $I_n^0=GTJ_n^0$:

$$I_n^0=2\pi n,\ n-\text{integer}. \tag{2.4}$$

Let the system at $t=0$ be in the neighborhood of a resonance of number n. Then, when $K\ll 1$, to estimate the change in the action $I(t)$, we can neglect the influence of the rest of the resonances (keep in the summation in (2.2) only the term with number n). This approximation corresponds to the resonance Hamiltonian:

$$H_p=\frac{G}{2}(J-J_n^0)^2+\frac{\varepsilon}{T}\cos\psi_n,\quad \psi_n=\theta-n\nu t. \tag{2.5}$$

Equation (2.5) yields an estimate of the width of the resonance in terms of action:

$$\delta I_n=2|I_{\max}-I_n^0|=4(\varepsilon GT)^{1/2}. \tag{2.6}$$

We note that in this case δI_n does not depend on n, since all harmonics of the external force in (2.2) do not depend on the action, which is usually fulfilled only approximately.

An approximate criterion for transition to global chaos can be derived from the condition of interaction (overlap) of the primary resonances. For the system of (2.1) the distance in terms of action between the nearest primary resonances is

$$\Delta I_n\equiv|I_{n+1}^0-I_n^0|=2\pi\ (n=0,\pm 1,\ldots). \tag{2.7}$$

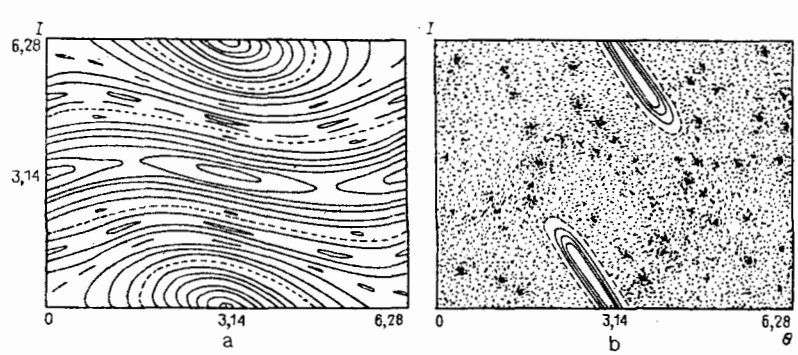

FIG. 1. Phase plane of the standard mapping. a–$K=0.6$. b–$K=4.2$.

Let us introduce the Chirikov parameter of overlap of nonlinear resonances,[3,4] which in this case can be represented in the form

$$\bar{K} = \frac{\delta I}{\Delta I} = \frac{2}{\pi}(\varepsilon G T)^{1/2} = \frac{2}{\pi}K^{1/2}. \tag{2.8}$$

When $\bar{K} \ll 1$ ($K \ll 1$), the motion is locally regular, while when $K \gtrsim 1$ a transition occurs to global chaos. As we see from (2.8), the relationship holds that $\bar{K}^2 \approx K$, which, as a rule, is maintained in the more general case.[3,5] The fundamental properties of the system of (2.1) in the region of strongly developed chaos ($K \gg 1$) can be represented as follows:[5]

1) Local instability of trajectories:[4)]

$$|\delta\theta_n/\delta\theta_0| \sim K^n = \exp(nh_0). \tag{2.9}$$

The increment $h_0 = \ln K$ is proportional to the maximum Lyapunov index, while the average value of h_0 over the phase space is known as the Kolmogorov entropy (Ref. 7, Ch. 5.2).

2) Decay of phase correlations of the type of

$$R_n = \frac{1}{2\pi}\int_0^{2\pi} \exp(i\theta_n)d\theta_0 \sim \exp(-nh_0/2). \tag{2.10}$$

3) Diffusional increase in the mean energy of the system:

$$\overline{I_n^2} \approx \overline{I_{n-1}^2} + \frac{K^2}{2} = I_0^2 + \frac{K^2}{2}n, \tag{2.11}$$

Here the bar denotes averaging over the ensemble of trajectories. All the properties 1–3 can be manifested in magnetic systems (see Sec. 5).

2.2. Chaos in dissipative systems. Strange attractor. Fractal dimension

In dissipative systems the phase volume contracts. In this way dissipative systems differ from Hamiltonian systems in which, according to the Liouville theorem, the phase volume is conserved. Owing to this contraction, the phase trajectory is drawn toward a certain set of points called the attractor. For a steady state the attractor is a point (node or focus) having the dimension zero. In periodic motion the attractor (or limit cycle) has the dimension unity. In the case of quasiperiodic motion with two incommensurate frequencies, the trajectory amounts to an unclosed spiral and shrinks down to a two-dimensional torus. If there are n incommensurate frequencies, then the attractor has the form of an n-dimensional torus. An attractor corresponding to steady-state chaotic motion is called a strange or stochastic attractor. Let us examine how a strange attractor arises using the example of the dissipative standard transformation (Ref. 5, supplement 3).

The equations of (2.2) generalized to the case of finite dissipation have the form

$$\dot{J} = -\gamma(J - J_0) + \varepsilon T \cos\theta \cdot \delta_T(t), \tag{2.12}$$

$$\dot{\theta} = \omega(J), \quad \omega(J) = \omega_0\left(1 + \alpha\frac{J - J_0}{J_0}\right).$$

In (2.12) J_0 is the action corresponding to a stable cycle with $\varepsilon = 0$. The condition $J_0 \neq 0$ implies that, when $\varepsilon = 0$ in the initial physical system, a mechanism of pumping energy also exists besides dissipation. The discrete mapping corresponding to (2.12) has the form

$$y_{n+1} = \exp(-\Gamma)(y_n + \varepsilon\cos 2\pi x_n),$$
$$x_{n+1} = x_n + \frac{\omega_0 T}{2\pi}(1 + \alpha\mu y_n) + \frac{K_0\mu}{2\pi}\cos 2\pi x_n \pmod 1, \tag{2.13}$$

Here we have $y_n = (J_n - J_0)/J_0$, $x_n = \theta_n/2\pi$, $\Gamma = \gamma T$, $\mu = [1 - \exp(-\Gamma)]/\Gamma$, $K_0 = \varepsilon\alpha\omega_0 T$. When $\Gamma \to 0$, the mapping (2.13) goes over into the standard mapping of (2.3). Equation (2.13) implies that $|\delta x_{n+1}/\delta x_n - 1| \sim K_0\mu|\sin 2\pi x_n|$. Therefore the condition of local instability can be represented in the form

$$K = K_0\mu = (K_0/\Gamma)[1 - \exp(-\Gamma)] \gg 1. \tag{2.14}$$

In this case the mapping of (2.13) leads to a strange attractor, whose form is shown in Fig. 2. When $\Gamma = 0$ the condition (2.14) is reduced to the condition of strong chaos in the dissipation-free case, $K_0 \gg 1$. We must note that, for the mapping of (2.13), as for the standard mapping (2.3), the following conditions hold: 1) local instability of motion; 2) decay of the phase correlation functions; 3) a continuous frequency spectrum of the motion. The geometric structure of the strange attractor possesses scale invariance, repeating itself on ever smaller scales. Such structures—fractals—have a fractional dimension called a fractal dimension.[14,15] A mathematically correct definition, which allows extension of the concept of dimension from integers (corresponding to points, lines, surfaces, etc.) to fractions is the definition of the dimensionality of a set according to Hausdorff:

$$d_H = \lim_{\varepsilon\to 0}\frac{\ln N(\varepsilon)}{\ln(1/\varepsilon)}. \tag{2.15}$$

In (2.15) ε is the dimensionless length of an element covering the set (e.g., a cube), and $N(\varepsilon)$ is the number of elements necessary to cover the set being studied.

Examples of calculation of the dimensions of different fractal sets according to the definition (2.15) are given, e.g., in Ref. 7, Chap. 3; Ref. 6, Chap. 7. For small decay $\Gamma \ll 1$ and developed chaos $K \gg 1$, the dimension of the strange attractor in the Zaslavskiĭ mapping is close to two: $d_H \approx 2 - \Gamma/\ln K$.[5]

We must note that the definition of dimension according to Hausdorff in (2.15) is difficult to use in processing experimental data, since it requires excessive computer calculations. Therefore, in practice one often applies other methods that enable one to estimate the fractal dimension of the strange attractor. Most often one uses the method of the

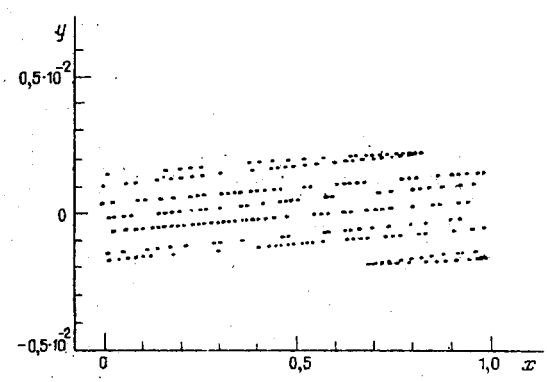

FIG. 2. Zaslavskiĭ's strange attractor ($K = 9.03, \Gamma = 5$). (Ref. 5).

correlation integral (Ref. 7, Chap. 5), which one can use to determine rather quickly a lower bound of the Hausdorff dimension (this method has been used, e.g., in Refs. 37 and 38 to determine the dimension of a strange attractor in experiments on parametric excitation of spin waves in magnetics).

In the general case a dynamical system can have not one, but several attractors of different types. The character of the motion that is established in such a case in the system will depend on the attractor to which the trajectory will be attracted under the given initial conditions. When the region of attraction (the so-called basin of the attractor) of a simple attractor overlaps part of a strange attractor, it becomes metastable.[15] In this case, in the course of a certain time (as a rule rather long), the trajectory lies on the strange attractor and the motion becomes chaotic. Then the trajectory goes over into the region of the simple attractor and steady-state regular motion is established. Such an effect has been called the crisis of a strange attractor.[15]

All the concepts introduced in this section arise in the treatment of dissipative chaos in magnetic systems.

2.3. Transition to chaos through a period-doubling bifurcation and alternation

At present rather many different scenarios of transition to chaos are already known, which are realized in different physical systems.[6,7,15] Here we shall study in greater detail two such scenarios that are most often encountered in magnetic systems.

2.3.1. Period-doubling bifurcations

Let a single dynamic variable $x(t)$ exist, which is examined at discrete instants of time n. We shall assume that the equations of motion can be reduced to the mapping:

$$x_{n+1} = f_r(x_n), \tag{2.16}$$

Here f_r is a certain function, and r is a parameter. For definiteness we shall choose f_r in the form $f_r(x) = rx(1-x)$. The mapping of (2.16) with this form of f is called the logistic mapping, and a detailed analysis of it is given in Ref. 7, Chap. 3. When $r<1$ this mapping has only one stable stationary point[5)] $x_1^* = 0$ toward which the trajectory is attracted. When $1<r<3$, the point x_1^* becomes unstable and a new stationary stable point appears, $x_2^* = 1-(1/r)$. When $r = r_1 = 3$ this point also becomes unstable and a new stationary stable point appears, $x_2^* = 1-(1/r)$. When $r = r_1 = 3$ this point also becomes unstable and stable motion arises with period 2, which corresponds to two stationary points $\bar{x}_1$ and $\bar{x}_2$ of the mapping $f_r^2(x) \equiv f_r[f_r(x)]$. Such a bifurcation is called a period-doubling bifurcation (Fig. 3). Here any sequence of iterations of the mapping is attracted as $n\to\infty$ to the points $\bar{x}_1$ and $\bar{x}_2$ (Fig. 4). When $r = r_2 > r_1$ one observes the next period doubling. Feigenbaum[16] found that the values of r_m at which period-doubling of the mth order occurs satisfy the relationship

$$\frac{r_m - r_{m-1}}{r_{m+1} - r_m} \to \delta \equiv 4{,}6692\ldots, \quad m\to\infty, \tag{2.17}$$

or

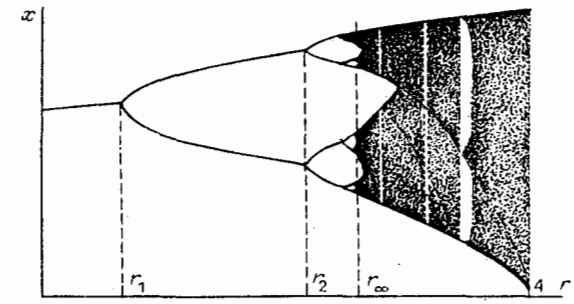

FIG. 3. Bifurcation diagram for the logistic mapping.[7]

$$\Delta r_{m+1} = \delta^{-1}\Delta r_m \ (m\to\infty), \quad \Delta r_m \equiv r_m - r_{m-1}.$$

The expression (2.17) means that the "bifurcation intervals" decline exponentially with increasing m. When $r > r_\infty \approx 3.5699\ldots$, chaos arises. However, even in this region at certain values of r the motion is regular—these are the so-called windows of regularity (see Fig. 3). For the logistic mapping, windows of regularity are observed for which the motion is periodic with periods $p = 3$, 5, and 6. The transition from a window of regularity to chaos can also occur through period-doubling bifurcations with universal laws of the type of (2.17). The relationship (2.17) is universal in the sense that it holds for an entire class of mappings of the form of (2.16) for which the function f has a quadratic maximum.

The doubling bifurcations that we have examined are often observed in magnetic systems. An analog of the parameter r in this case is, for example, the pump power in ferromagnetic resonance (see Sec. 3). Usually in real experiments one cannot trace a large number of doubling bifurcations owing to the property of exponential decline of the magnitude of Δr_m. Therefore, already after several bifurcations the system goes over into chaos.

2.3.2. Transition to chaos via alternation

Alternation means the existence of rather long time intervals of motion with regular behavior, interrupted by random beats. An example of such behavior for the logistic mapping is shown in Fig. 5. When $r = r_c \equiv 1 + 8^{1/2}$, one observes a window of regularity with period 3 (Fig. 5a). When r is a little smaller than r_c, alternation arises (Fig. 5b). The reason for such behavior consists in the fact that the system near r_c conserves memory of the vanished stable stationary point, alongside which the motion is strongly retarded, so

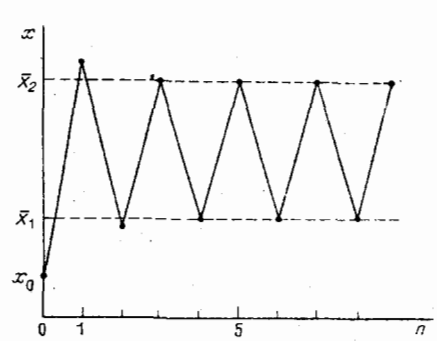

FIG. 4. Form of the iterations of the initial point when the mapping has an attractor of period 2. (Ref. 7).

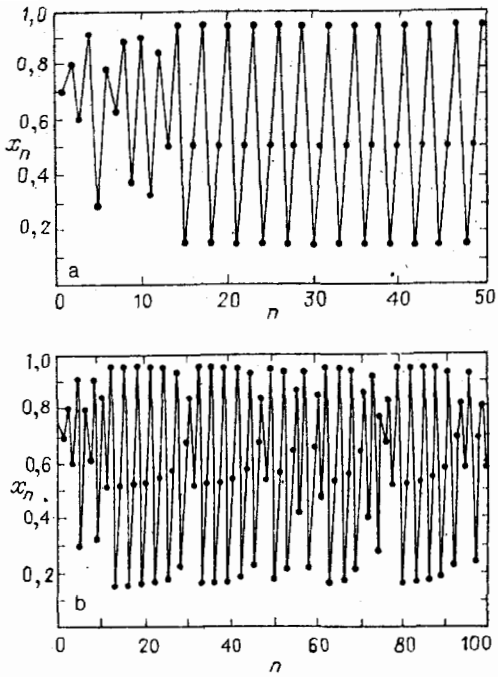

FIG. 5. Form of the iterations of the logistic mapping for $r_c - r = -0.02$ (stable cycle of period 3) (a) and $r_c - r = 0.02$ (alternation) (b). (Ref. 7).

that the system departs for a long time from the laminar phase of motion (Ref. 7, Chap. 4). The mean duration of regular motion as a function of the distance from the critical point has the form[17]

$$\bar{t}_{\rm reg} \propto |r - r_c|^{-1/2}. \tag{2.18}$$

The features described above of the transition to chaos in Hamiltonian and dissipative systems are illustrated using the example of very simple mappings. Naturally, the fundamental properties of chaos in mappings extend to continuous systems. However, discrete mappings not only are far simpler to study analytically and numerically, but mappings often arise naturally in experimental situations. This is possible when a periodic sequence of short pulses acts on a system, and also when one is studying successive intersections of the phase trajectory of some hypersurface in phase space (Poincaré section). In an experiment one most often studies the dependence of the intensity of the $(n+1)$th peak of the real signal V_{n+1} on the intensity of the nth peak V_n (reverse mapping). Such a construction fixes the mapping on the Poincaré section as determined by the condition that the given coordinate should be maximal in phase space.

3. CHAOS IN THE PARAMETRIC EXCITATION OF SPIN WAVES

At present the greatest number of studies on magnetic chaos are devoted to the theoretical and experimental study of chaos in the parametric excitation of spin waves in magnetically ordered materials. As we see from the preceding discussion, the transition to chaos, even in the simplest cases, occurs via a sequence of various types of preliminary instabilities (bifurcations). Typical instabilities of this type in magnetic systems are the Suhl instabilities,[18] which are manifested in the creation of wave motions of magnetization upon increasing the pumping energy into the system. Upon further increase of the pump power, such regular motions as have already arisen prove generally to be unstable with respect to creation of new low-frequency motions and chaos. This scenario of transition to chaos in magnetic systems differs to a considerable extent from the pattern of weak turbulence of spin waves.[19,20] In the latter case a large number of weakly nonlinear waves is excited, the interaction among which leads to chaotization of their phases and to the possibility of using the kinetic approach in describing magnetic turbulence. However, such a pattern of excitation and interaction of waves is not always realized. References 21 were devoted to problems of the stability of weakly turbulent spectra and the accompanying phenomena that arise here. Here there is no need to dwell on the details of the different approaches to studying the dynamical properties of magnetic systems. A detailed review of the results existing in this field is contained in Refs. 19 and 20. We shall present only some characteristic properties of Suhl instabilities, which in a number of experiments are typical preliminary instabilities on the road to chaos.

3.1. Suhl instabilities

Usually the theory of the parametric excitation of magnetically ordered materials is constructed on the basis of concepts of elementary excitations—magnons or spin waves. The Hamiltonian of the system has the form

$$H = H_0 + H_p + H_{\rm int}; \tag{3.1}$$

$H_0 = \Sigma\omega_k a_k^* a_k$ describes the free spin waves (a_k and a_k^* are the complex amplitudes of the waves); H_p is the parametric interaction of the magnons with the external field; $H_{\rm int}$ describes the nonlinear interaction of the magnons. One takes account of the linear decay of the waves by introducing into the equations of motion terms containing $\gamma_k a_k$ (γ is the decrement):

$$i\dot{a}_k = \frac{\partial H}{\partial a_k^*} - i\gamma_k a_k. \tag{3.2}$$

The Hamiltonian H_p has a different form in the cases in which the alternating field $h(t) = h_0 \exp(-i\omega_p t)$ is perpendicular or parallel to the constant field H_0 (transverse and parallel pumping of spin waves).

3.1.1. Transverse pumping of spin waves. Suhl instabilities of the first and second kinds

In transverse pumping the interaction of the magnons with the field is described by the following Hamiltonian:[18]

$$H_p = Vh_0[a_0 \exp(i\omega_p t) + \text{c.c.}]. \tag{3.3}$$

Here we have $V = g(SN/2)^{1/2}$, where g is the gyromagnetic ratio, and N is the total number of spins S in the system. At low levels of excitation homogeneous resonance arises under the action of the pump of (3.3). As Suhl first showed, as the amplitude h_0 increases, the interaction of the homogeneous mode a_0 with the inhomogeneous mode a_k leads to the appearance of inhomogeneous spin waves. If the fundamental role in the interaction is played by three-wave processes with $H_{\rm int} \sim \Sigma(U_{0,k,-k} a_0^* a_k a_{-k} + \text{c.c.})$, then the homogeneous precession breaks down into two magnons with momenta $\mathbf{k}$ and $\mathbf{k}'$ and energies $\hbar\omega_k = \hbar\omega_p/2$. Such a process is called Suhl instability of the first kind. The threshold of this process is determined by the expression (Ref. 20, Sec. 14):

$$|U_{0,k,-k}|a_{th}(k, h_0) = \gamma_k. \tag{3.4}$$

The groups of spin waves with the defined direction **k** (Ref. 20, Sec. 14) have the maximum coupling with the pump (minimum excitation threshold a_{th}). The critical value of the field $h_{0,th}$ can be very small, and for YIG crystals can amount to 10^{-3}–10^{-1} Oe, depending on the detuning of the pump frequency from the ferromagnetic resonance frequency.[20]

As H_0 is increased or ω_p is decreased, the situation can be attained that three-wave decay processes will be forbidden. However, if four-wave processes are allowed, then Suhl instability of the second kind is easily realized: $2\omega_p = \omega(\mathbf{k}) + \omega(-\mathbf{k})$. This process can be effected as follows: the external field excites homogeneous precession at resonance $\omega_p \approx \omega_0$, and then a four-magnon parametric process occurs: $2\omega_p = \omega(\mathbf{k}) + \omega(-\mathbf{k})$. The threshold of this process is minimal at points on the resonance surface $\theta_k = 0, \pi$ (θ is the angle between **k** and $\mathbf{H}_0$).

3.1.2. Instability in parallel pumping of spin waves

The Hamiltonian of the interaction of a system of magnons with the alternating field $h(t)$ parallel to the constant field has the form[19,20]

$$H_p = \frac{1}{2}\sum_k [h_0 V_k a_k a_{-k} \exp(i\omega_p t) + \text{c.c.}]. \tag{3.5}$$

Here we have $V_k = g\pi M \sin^2\theta_k/\omega_k$, M is the saturation magnetization, and θ_k is the angle between **k** and **H**. In this case the threshold of parametric instability is determined by the expression

$$h_{0,th} V_k = \gamma_k. \tag{3.6}$$

The threshold is minimal for magnons of frequency $\omega_k = \omega_p/2$ and with $\theta_k = \pi/2$. The magnitude of the threshold field $h_{0,th}$ for parallel pumping coincides in order of magnitude with the threshold field for transverse pumping far from ferromagnetic resonance.

Now let us proceed to study chaotic dynamics in the parametric excitation of spin waves.

3.2. Theoretical models

3.2.1. Parallel pumping

The possible existence of a strange-attractor regime in the parametric excitation of spin waves was first demonstrated in the study of Astashkina and Mikhaĭlov.[22,6)] The following model was treated: parallel pumping excited parametrically in an antiferromagnet a pair of primary spin waves with wave vectors $\pm\mathbf{k}_0$, each of which in turn breaks down into two secondary waves with wave vectors $\pm\mathbf{k}_1$ and $\pm\mathbf{k}_2$. The authors of Ref. 22 chose the Hamiltonian of the system in the form

$$\begin{aligned} H = {} & \omega_{k_0}(|A_{k_0}|^2 + |A_{-k_0}|^2) + [h_0 V \exp(-i\omega_p t) A^*_{k_0} A^*_{-k_0} + \text{c.c.}] \\ & + \frac{1}{2}T(|A_{k_0}|^4 + |A_{-k_0}|^4) + 2S|A_{k_0}|^2|A_{-k_0}|^2 \\ & + \frac{1}{2}(\Phi A_{\pm k_0} a^*_{\pm k_1} a^*_{\pm k_2} + \text{к.с.}) + \omega_{k_1}|a_{\pm k_1}|^2 + \omega_{k_2}|a_{\pm k_2}|^2. \end{aligned} \tag{3.7}$$

In addition to the parametric excitation by the external field $h(t) = h_0 \exp(-i\omega_p t)$ of the primary waves (with amplitudes A) and their decay into secondary waves (with amplitudes a), this Hamiltonian also describes processes of nonlinear interaction between the primary waves (T and S are the amplitudes of the interaction). Here the resonance conditions are satisfied: $\mathbf{k}_0 = \mathbf{k}_1 + \mathbf{k}_2$, $\omega_{k_0} = \omega_{k_1} + \omega_{k_2}$. The damping of the waves was taken into account in the equations of motion [see (3.2)]; it was assumed that $\gamma_{k_{1,2}} = \gamma_{k_0} \equiv \gamma$. Under some simplifying assumptions that were confirmed in a numerical experiment, a system of four real differential equations was derived in Ref. 22, and its stability was analyzed. Upon variation of the parameter

$$x_0 = [(h_0/\gamma|V|)^2 - 1]^{1/2}, \tag{3.8}$$

which characterizes how far the threshold of parametric instability ($x_0 = 0$) is exceeded for the primary waves $A_{\pm k_0}$, one observes the following sequence of bifurcations. When $0 < x_0 < x_1 \equiv 2|S|\gamma/|\Phi|^2$, a stable stationary point P exists in phase space (a stable focus), to which the phase trajectories are attracted. This regime corresponds to excitation of primary spin waves with $A_{\pm k_0} \neq 0$ and to absence of secondary waves ($a_{\pm k_{1,2}} = 0$) for which the primary waves are the pumping source. The value $x_0 = x_1$ defines the threshold for creation of secondary waves. When $x_0 = x_1$ the point P loses stability and a stationary stable point $\overline{P}$ arises. In this regime the amplitude of the primary waves is frozen at the level $|A^{(0)}_{\pm k_0}| = (\gamma/|\Phi|)^2$ and the steady-state value of the amplitudes of the secondary waves $a_{k_{1,2}} \neq 0$ is maintained owing to the energy flux from the primary waves. As x_0 increases further up to some level, the point $\overline{P}$ becomes unstable, and a limit cycle arises. The onset of this instability involves the fact that the primary waves, through which energy is transmitted from the external pump to the secondary waves, are not able to transmit a very large energy flux, keeping their amplitudes frozen thereby at the level $|A^{(0)}_{\pm k_0}|$. With a further increase in x_0, as numerical experiment showed, the limit cycle breaks down. Here the system goes over into chaos (Fig. 6). A calculation was performed[22] of the magnitude of the maximum Lyapunov exponent λ as a function of the parameters of the system. The value of λ reached a maximum at $x_0 \approx 4x_1$. When $x_0 > 6x_1$, an alternation was observed of stable limit cycles and regions of chaotic behavior. The authors of Ref. 22 advanced the hypothesis that the dynamical chaos that they had discovered in the simple model

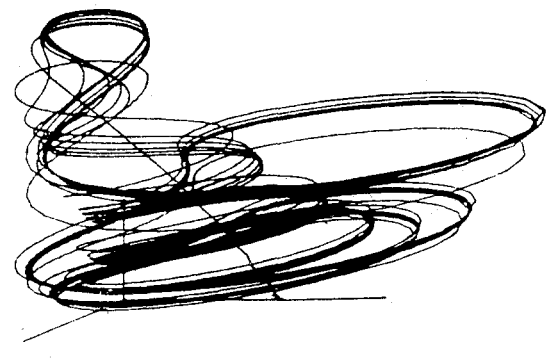

FIG. 6. Form of the phase trajectory in chaotic motion ($x_0 = 4x_1$) in the model of Astashkina and Mikhaĭlov.[22]

system of (3.7) can take place in various ferromagnets and antiferromagnets under various methods of excitation and will draw attention to the study of chaotic oscillations in the parametric excitation of spin waves in magnetically ordered crystals. This prediction has been fully confirmed.[23-42]

We must note that the transition to chaos described in Ref. 22 can occur when the decay of the parametrically excited spin waves into two spin waves, into a paired spin wave and a phonon, or into two phonons, is allowed by the conservation laws. However, in magnetically ordered materials one often encounters a situation in which such processes are forbidden and contribute only to the damping of the spin waves. If four-wave processes are allowed, then in this case the Hamiltonian has the form (3.1), (3.5), and[9,20]

$$H_{\text{int}} = \frac{1}{2}\sum_{k,k'} (S_{kk'} a_k^* a_{-k}^* a_{k'} a_{-k'} + 2T_{kk'} a_k^* a_{k'}^* a_k a_{k'}). \qquad (3.9)$$

It was shown numerically in Refs. 23 that in this situation chaos can also occur. A very simple model was proposed in Ref. 23 that took account of only two modes with wave vectors directed perpendicular to the field. It was also assumed that all the coupling coefficients of the field with the waves V_{k_1} and V_{k_2}, of the nonlinear interaction of the spin waves $T_{k_1k_2}$ and $S_{k_1k_2}$, and of damping γ_k are the same for both waves, and the detunings of the frequencies of the waves from the pump frequency ω_p coincide: $\Delta\omega_1 \equiv (\omega_{k_1} - \omega_p/2) = \Delta\omega_2 \equiv (\omega_{k_2} - \omega_p/2) \equiv \Delta\omega$. Such a symmetric model is the simplest one in which chaos can occur with parallel pumping.

The magnetization and the absorption are expressed in terms of pair correlators of the form $n_j = \langle a_{k_j}^* a_{k_j}\rangle$ and $\sigma_j = \langle a_{k_j} a_{-k_j}\rangle \exp(i\omega_p t)$ $(j = 1,2)$. The problem of the theory actually reduces to writing the kinetic equations for these quantities. It was shown[23] that the solutions of these equations describe stationary states, periodic motion, period doubling, and chaos. There are three types of stationary points: 1) $n_1 = n_2 = \sigma_1 = \sigma_2 = 0$; 2) $n_i = \sigma_i = 0$, $n_j \neq 0$, $\arg \sigma_j \neq 0$ $(i \neq j)$; 3) $n_1 = n_2 \neq 0$, $\arg \sigma_1 = \arg \sigma_2 \neq 0$. Above the threshold of Suhl instability (3.6) the trivial stationary point of type 1 becomes unstable. When $1 \leqslant h_0 V/\gamma < 4$, the trajectories are attracted to the stationary points of types 2 and 3. When $h_0 V/\gamma \geqslant 4$, limit cycles arise. Here a hysteresis phenomenon can occur, in which, at a fixed h_0, depending on the initial conditions, the trajectories are attracted either to a limit cycle or to a stable state. With further increase in h_0, a sequence of period doubling of the oscillations was observed, which led to chaos (a strange attractor) at $h_0 V/\gamma \approx 5.53$. The similarity parameter $\delta \approx 4.675$ determined numerically proved to be very close to the universal Feigenbaum parameter for one-dimensional mappings in (2.17).

An "asymmetric" generalization of the two-mode model has been discussed in Ref. 24. The existence of different parameters for each of the waves can, in particular, lead to the appearance of other "subharmonic" scenarios of the transition to chaos that differ from period doubling. Experimentally such scenarios, just like the Feigenbaum scenario, have been observed in crystals of yttrium iron garnet (YIG).

3.2.2. Transverse pumping

A theoretical study of the transition to chaos in transverse pumping was first carried out in Refs. 25–27. The

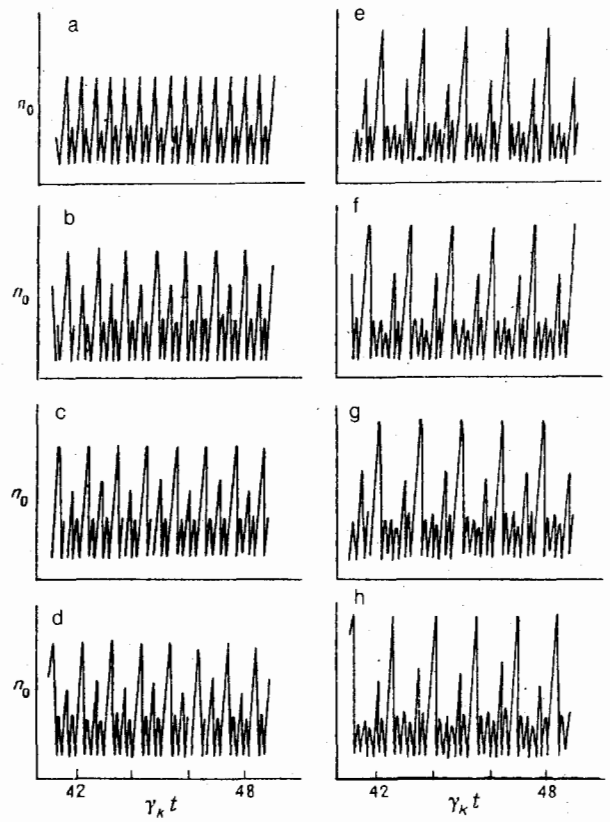

FIG. 7. Bifurcations of the oscillations of the density of magnons of the homogeneous mode n_0 with increase in the pump power $r = h_0/h_{0,\text{th}}$. a–Period 1 ($r = 7.36$), b–Period 2 ($r = 7.64$), c–Period 4 ($r = 7.72$), d–Onset of chaos ($r = 7.77$), e–Period 3 ($r = 8.197$), f–Period 6 ($r = 8.21$), g–Period 12 ($r = 8.22$), h–Chaos ($r = 8.24$). (Ref. 27).

Hamiltonian of the system has the form of (3.1), (3.3), and (3.9). References 25–27 proposed and analyzed a very simple model in which a homogeneous mode with $k = 0$ is coupled only with a paired mode with wave vectors k and $-k$. Numerical analysis of such a system showed that a strange attractor arises upon excitation above the threshold of Suhl instability of the second kind. These theoretical studies were conducted in connection with an attempt to explain the pioneering experiments of Gibson and Jeffries,[34] and the values of the parameters were selected from these considerations. The obtained results agree qualitatively with the experimental results (see the following section on the possibility of quantitative comparison). In the numerical simulation in Refs. 26 and 27 a transition to chaos was observed via period doubling (Fig. 7a–d), with a similarity parameter $\delta \approx 4.53$. With increasing field a window was observed with a period of $3T \times 2^n$ (Fig. 7e–h). The reverse mapping[27] proved to be similar to that found experimentally.

Under conditions of an experiment to observe spin-wave chaos, the magnetic specimen is placed in a resonator. Naturally the presence of the resonator can substantially affect the nonlinear dynamics. References 28 and 29[7)] were devoted to taking account of the effect of electromagnetic modes on the spin modes. The presence of the electromagnetic modes led to the appearance of a new transition to chaos via "oscillations with irregular periods".[28]

The case of an arbitrary "oblique pumping" of spin waves[8)] was studied in Ref. 30 (here also the electromagnetic modes of the resonator were taken into account). In this

TABLE I.

Substance	Type of excitation, type of instability	Pump frequency, GHz	H, kOe	T, K	Dimensions, mm	Characteristic frequency of nonlinear oscillations	Year	Reference
Ga-YIG and YIG	$\mathbf{h}(t) \perp \mathbf{H}$, instability of the 2nd kind	1,3	0,46	300	Sphere $R = 0{,}47$	$f = 250$ kHz $f = 16$ kHz	1984	[34]
YIG	$\perp$, 1st kind	9,2	≤ 4	300	Sphere $R = 0{,}33$	16 kHz $10^4 - 10^6$ Hz	1988	[30]
YIG	$\perp$, 1st kind	2,5	0,76	300	Sphere $R = 10$	5 — 400 kHz	1987	[39]
YIG		9,4	1,54	300	Spheres and disks $R = 1$	50 — 300 kHz	1986	[24]
YIG	$\parallel$	8,86	1,935	4,2	Disk $R = 0{,}64$, $H = 0{,}4$	—	1986	[35]
$CsMnF_3$	$\parallel$	18	1,5 — 2,5	1,4 — 1,6	Cylinder $R = 1$, $H = 1$	~ 100 kHz	1986 1988	[41] [42]
$CuCl_2 \cdot 2H_2O$	$\parallel$	8,91	6,3	1,4	1,1×1,5×3,9	35 MHz	1984	[36]
$(CH_3NH_3)_2CuCl_4$	$\parallel$	9,4	1,05 + 1,15	1,65	Disk $R = 4{,}5$, $H = 0{,}15$	8 kHz	1986 1987	[37] [38]
$[NH_3(CH_2)NH_3]CuCl_4$	$\parallel$	9,36	8,9	1,7	—	~ 1 MHz	1986	[29]
$(C_2H_5NH_3)_2MnCl$	$\perp$	70	7 — 9	< 2,2	—	2 — 5 kHz	1989	[40]

study also an attempt was undertaken to extend the two-mode approximation further. It was shown that taking account of a third mode leads, in particular, to the appearance of a quasiperiodic scenario of transition to chaos.[30] Recently a theorem was proved[30] under rather general conditions that states that the solutions of the dissipative Landau-Lifshits equation have an attractor of finite dimension. This theorem implies that, after some "transition time", a finite number of modes suffices for describing spin-wave turbulence. However, this theorem does not allow one to predict reliably the number of necessary modes. Therefore this question remains essentially open (see also the discussion in Refs. 32 and 33).

3.3. Discussion of experiments

Starting with the pioneering study of Gibson and Jeffries,[34] in which transition to chaos via period-doubling bifurcations was first observed, up to now already rather many experiments have been performed on various magnetic materials, in which a variety of approaches to chaos in the para-

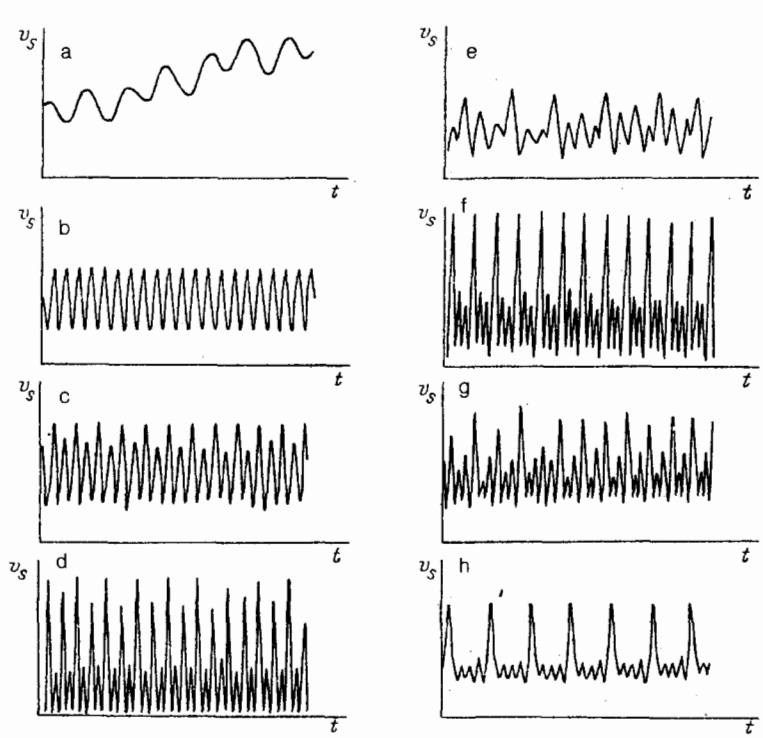

FIG. 8. Types of oscillations in the experiment of Gibson and Jeffries.[34] a–Auto-oscillations with frequency $f_1 \approx 250$ kHz. b–$f_2 \approx 16$ kHz. c–Bifurcation $f_2/2$. d–Bifurcation $f_2/4$. e–Chaos. f–Period 3. g–Bifurcation to period 6. h–Period 4, differing from r.

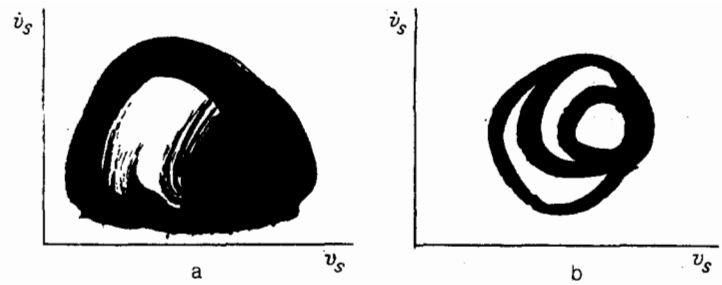

FIG. 9. Phase portrait in the coordinates of the signal (V_s) against its derivative ($\dot{V}_s$). a–Chaos[34]. b–Auto-oscillations with period 3.

metric excitation of spin waves was demonstrated (see Table I).

3.3.1. Chaos in Suhl instability of the second kind in YIG doped with gallium

Owing to its record-making low damping of spin waves, high Curie temperature, and excellent crystal quality, YIG has always been the most popular object in studies of parametric resonance. The use in Ref. 34 of gallium-doped YIG, which has a lower magnetization than pure YIG, enabled lowering the resonance field and the resonance frequencies. Chaos was not observed in the case of parallel pumping, apparently owing to the insufficiently high power of the alternating field that was used. For this reason the fundamental measurements were performed under conditions of Suhl instability of the second kind.

A rich pattern was observed of complex oscillatory regimes and transitions among them: stationary states, oscillations with a period of 250 kHz and then 16 kHz, sequences of period doubling, chaos, windows with periods of 3 and 5, and doubling of these periods. Some of the results are presented in Figs. 8 and 9. The analysis demonstrated the varied structure of the strange attractor. In particular, the reverse mapping constructed from the data of Fig. 8e has the form of a quadratic parabola and is well simulated by the one-dimensional logistic mapping (see Sec. 2.3).

Under supercritical conditions that exceeded the threshold value by about a factor of 30 ($h_0/h_{0,\text{th}} \approx 30$), auto-oscillations arose with the frequency $f \approx 250$ kHz. With increasing h_0 the amplitude of these oscillations declined, and when $h_0/h_{0,\text{th}} \approx 31$, new oscillations appeared with the frequency $f_2 \approx 16$ kHz (Fig. 8a,b). The nature of these oscillations has aroused discussion in the literature. Therefore we should discuss them in greater detail.

Let us start with the concept of the authors of the experiment. Owing to the finite width of the lines of homogeneous resonance, the broadened homogeneous mode can excite a wave packet of width $\Delta\omega_k$ that moves as a whole with the velocity $d\omega_k/dk$. In a sphere of radius R the minimum momentum of the standing wave is $\Delta k = \pi/R$, while the corresponding frequency of auto-oscillation is $\Omega = (\pi/R)\mathrm{d}\omega_k/\mathrm{d}k)$. In the case being discussed the dispersion law has the form

$$\omega_k^2 = (\omega_0 - \omega_m/3 + gDk^2)(\omega_0 - \omega_m/3 + gDk^2 + \omega_m \sin^2\theta_k). \tag{3.10}$$

Here we have $\omega_m = g \cdot 4\pi M = 5.27 \cdot 10^9\ \mathrm{s}^{-1}$, $g = 17.58 \cdot 10^6$ $(\mathrm{Oe \cdot s})^{-1}$, $\omega_0 = 8.16 \cdot 10^9\ \mathrm{s}^{-1}$, $D = 5.4 \cdot 10^{-9}$ $\mathrm{Oe \cdot cm^2}$. In Suhl instability of the second kind the threshold is minimal for waves with $\theta_k = 0$, and the corresponding frequency of the auto-oscillations is determined by the formula

$$f = \Omega/2\pi = (1/2R)\mathrm{d}\omega_k/\mathrm{d}k = (1/R)(gD\omega_m/3)^{1/2}. \tag{3.11}$$

When $R = 0.46$ mm, the frequency f_1 is approximately equal to 275 kHz, which is close to the experimental value of 250 kHz. The measurements performed on specimens with $R = 0.33$ mm showed that the frequency f_1 varied proportionally to R^{-1}. In the case of spheres of pure YIG with $R = 0.33$ mm, the measured frequency was $f \approx 900$ kHz, which is close to the value 920 kHz obtained from (3.11). Analogously an attempt was undertaken to explain the frequency $f_2 = 16$ kHz. However, in this case it was necessary to assume that waves were excited with $\theta_k = 60°$, since it is precisely for this value that the formula $f = (1/2R)\,d\omega_k/dk$ yields 16 kHz. On the other hand, the condition $\omega_{k=0} = \omega_p$ implies that $\theta_k = 60.4°$. Therefore the hypothesis was advanced that the wave vector of the corresponding waves is close to zero. Unfortunately there is no information on the behavior of the frequency f_2 as the parameters of the system are varied, e.g., R.

Another viewpoint on the nature of the auto-oscillations is presented in Refs. 24 and 25. It was assumed that one of the two observed frequencies arises as a bifurcation of creation of a cycle as a result of the nonlinear interaction between the homogeneous and inhomogeneous modes (see Sec. 3.2). However, numerical estimates were obtained two orders of magnitude larger than the actual values: 5.5×10^6 Hz,[24] and 0.9×10^6 Hz.[25]

3.3.2. Chaos in Suhl instability of the first kind in YIG

The dependence of the observed transitions to chaos on two parameters of the constant field, H_0 and the pumping power P_{in}, is shown in the diagram (Fig. 10).[30] We can see in this diagram: the threshold of Suhl instability with generation of one spin-wave mode of width < 0.5 G; auto-oscillations with a characteristic frequency of 10^4–10^5 Hz; transitions to chaos via period doubling and quasiperiodicity; rapid transition to turbulence with hysteresis; irregular relaxation oscillations and aperiodic pulsations. Most of these oscillations were observed in finite-mode models (see the previous section).

As has already been noted in Sec. 2.2, a strange-attractor crisis can occur. In the experiment of Ref. 39, above the threshold of Suhl instability of the first kind, a strange attractor was observed (with dimension ≈ 2.7), part of which intersected the basin of a simple attractor (nonchaotic) of dimension 4 or 5, depending on the pump power. The system

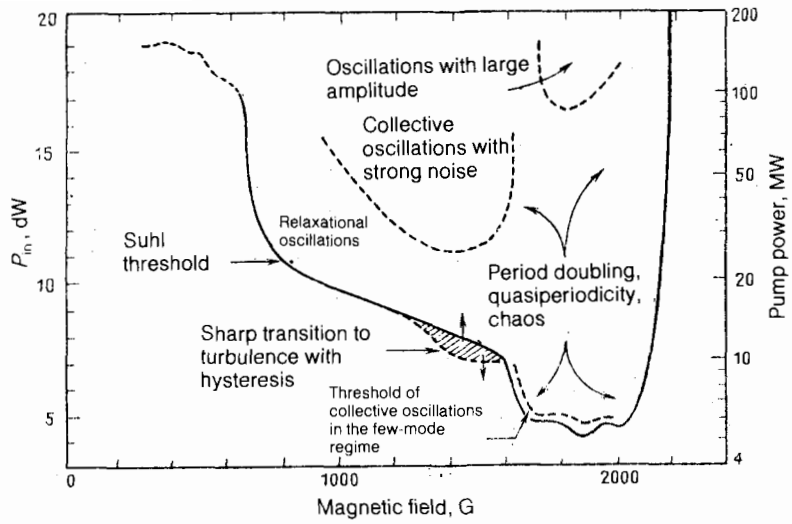

FIG. 10. Phase diagram.[30]

spent part of the time on the strange attractor, and then went over into the region of attraction of the periodic attractor. As a result the observed signal (Fig. 11) had the form of chaotic oscillations for the duration of the time t_{tr}, and then periodic oscillations were established exponentially rapidly. Here t_{tr}, which can be very large, depends as a power function on the reciprocal pump power.[39]

3.3.3. Chaos in YIG with parallel pumping

Chaos in YIG with parallel pumping has been studied by two groups.[24,26,35] In Refs. 24 and 26 the YIG spheres at room temperature were placed into a resonator of frequency $f = 9.4$ GHz. The alternating field was parallel to the constant field and parallel to the [111] axis. The constant field $H_0 = 1.54$ kOe was close to the curve $h_{0,th}(H_0)$ where waves were excited with $k \approx 0$ and $\theta_k = 0$. Auto-oscillations arose at $r = h_0/h_{0,th} = 1.5$. Their frequency ≈ 100 kHz increased linearly with increasing r. Period doubling occurred at $r = 1.62$, and then chaos set in without further doublings. Further, oscillations with the new frequency $f = 160$ kHz arose at $r = 1.84$, periods of $2T$ and $4T$ at $r = 1.04$ and 2.24, and then immediately periods of $3T$, $6T$, etc., and finally again chaos at $r = 3.43$. Moreover, for certain values of the direction and magnitude of the field a scenario was observed of the Feigenbaum type. The authors attribute such rather complex behavior of the system to the fact that it is really multidimensional and cannot always be described by a one-dimensional mapping.

In Ref. 35 experiments with disks were performed at liquid-helium temperature. Bifurcations were observed, $T \to 2T \to$ chaos, and reverse: chaos $\to 4T \to 2T \to T$. In this study the value of the Lyapunov exponent was determined from the experimental data: $\lambda \approx 0.34 > 0$.

3.3.4. Parallel pumping in the antiferromagnet $CuCl_2 \cdot 2H_2O$ (Ref. 36)

The first observations of period-doubling bifurcations in parametric excitation, besides the experiment with YIG,[34] were performed on the antiferromagnet $CuCl_2 \cdot 2H_2O$.[36] This crystal has not been studied as extensively as YIG, but the results that were obtained have a number of interesting features.

The specimens were kept at liquid-helium temperature, while parallel pumping was carried out in a pulsed regime with the parameters: rise time of the pulse = 20 ns, pulse duration = 10 ms, repetition frequency of pulses = 100 Hz. Oscillations of the imaginary component of the susceptibility were observed over a rather narrow interval of magnetic bias fields in the vicinity of the value 6.3 kOe with pumping of $P/P_{th} \approx 12$ dB. The dependence of the Fourier spectra on

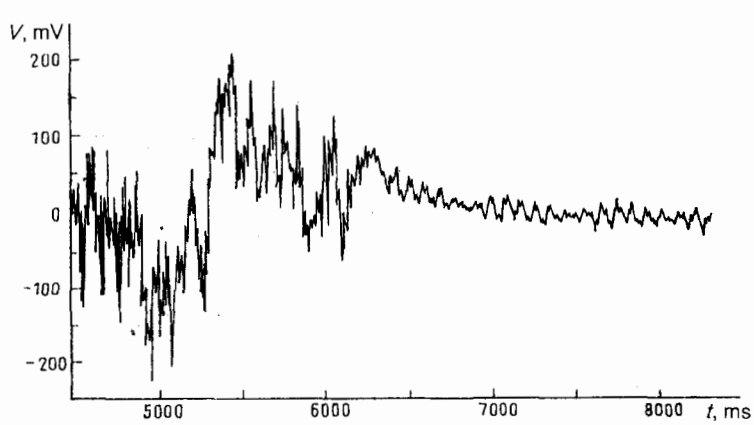

FIG. 11. Observed signal as a function of the time.[39]

the pumping level showed the appearance of a distinct peak at half the frequency ($T \to 2T$ transition) when the critical value was exceeded by $P/P_{th} \approx 14.4$ dB. For comparison the theory[23] yields $P/P_{th} = 14.66$ dB ($T \to 2T$), 14.87 dB ($2T \to 4T$), and 14.908 dB ($4T \to 8T$). Unfortunately, since the period of the oscillations ≈ 0.25 ms proved to be comparable to the pulse duration 10 ms, only damped oscillations were observed. Therefore it was possible to note only hints of quadrupling of the period, while the hypothesized further sequence of doubling bifurcations and chaos was not observed.

3.3.5. Layered magnetic materials

The layered magnetic materials $(CH_3NH_3)_2CuCl_4$, $(NH_3)_2(CH_2)CuCl_4$, and $(C_2H_5NH_3)_2MnCl_4$ are characterized by unusually weak relaxation and correspondingly a low level of threshold power. Therefore one can study these compounds in the far superthreshold region without fearing overheating of the specimens.

The ferromagnet $(CH_3NH_3)_2CuCl_4$ was the most thoroughly studied one.[37,38] Parallel pumping at the frequency 9.39 GHz was carried out at $T = 1.65$ K. Oscillations of different types were observed in the region of magnetic bias fields of 1050–1150 Oe. In particular, a transition to chaos was observed owing to the appearance of irregular peaks. In this case both the amplitude and the distance between peaks are irregular. Oscillations with an irregular period but practically with fixed amplitude were observed in the antiferromagnet $(NH_3)_2(CH_2)CuCl_4$ (Fig. 12).[29] The same type of oscillations were obtained in models that took account of the electromagnetic modes in the resonator.[28]

The fractal dimension was determined from the experimental data obtained in crystals of $(CH_3NH_3)_2CuCl_4$,[38] which increases with increasing pump level from 1.6 ± 0.4 to 3.4 ± 0.3. The authors of Ref. 38 consider a possible cause of the large error in determining the fractal dimension at pump levels near the threshold for forming a strange attractor to be the influence of noise and fluctuations in the experimental apparatus. Also the Lyapunov exponent and Kolmogorov entropy were calculated in this study. All these data indicate that dynamical chaos was actually observed in the case under discussion.

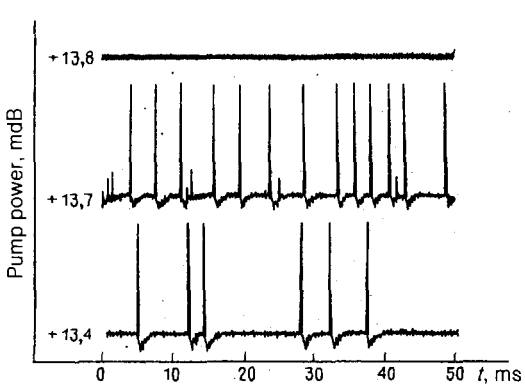

FIG. 12. Oscillations in the case of parallel pumping in $(NH_3)_2(CH_2)CuCl_4$. (Ref. 24).

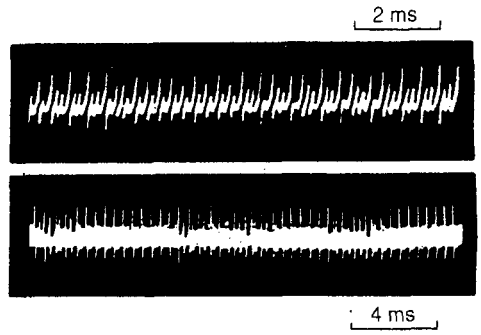

FIG. 13. Alternation of cycles of period 3. (Ref. 41).

3.3.6. The antiferromagnet $CsMnF_3$

The transition to chaos upon parallel pumping in $CsMnF_3$ at $T = 1.4$ K was studied in Refs. 41 and 42. Reference 41 studied the scenarios of the transition to chaos upon varying the constant magnetic field H_0 and the pump power P_{in}. In magnetic fields $H_0 < 2.3$ kOe a transition to chaos via period doubling was observed upon increasing P_{in}. This transition is close to the Feigenbaum scenario. Here windows of periodicity with periods of 3, 4, 5, and 7 were observed inside the region of chaos. When the pump power was maintained constant at a level insufficient for doubling of the fundamental period, the transition to chaos occurred at $H_0 > 2.3$ kOe by broadening of the fundamental line. A more detailed analysis enabled the conclusion that the transition to chaos in this case occurs via alternation (Fig. 13, cf. Fig. 5). The topology of the strange attractors that arise was studied in Ref. 42. It was shown that, in the range of the parameters P_{in} and H_0 near which the chaotic regimes develop through a cascade of period doubling, the complication of the regime (i.e., the increase of the amplitude of the chaotic component of the pulsations of magnon density) occurs with a constant number of degrees of freedom involved in the motion, and is accompanied by a complication of the topological structure of the strange attractors. In another scenario of the transition to chaos, a strange attractor is inserted into a space having a dimension that varies from 3 to 5, depending on the parameters of the system.

4. CHAOS IN NMR MASERS

Another example of a spin system in which a transition to dissipative chaos has been observed is the NMR maser or raser (raser–Radiowave Amplification by Stimulated Emission of Radiation). A raser consists of a nuclear spin system with negative polarization that interacts with an oscillatory circuit. The transition to chaos involves the modulation of one of the parameters of the system: the Q-factor of the circuit, the exciting field, the nuclear magnetization, or the width of the NMR line. Here, following Ref. 43, we shall study the latter case, which has proved very effective from the standpoint of the transition to chaos (for other results, see, e.g., Ref. 44 and the references cited therein).

In the experiments of Ref. 43 a high-quality ruby single crystal $Al_2O_3:Cr^{3+}$ was placed in a resonator. The observations were performed at $T = 1.6$ K with a constant field $H_0 = 1.1 \times 10^4$ Oe (NMR frequency in ^{27}Al $\omega_0/2\pi = 12$

MHz). A coil was wound around the specimen that was part of an oscillatory LC circuit with a frequency $\omega_{LC} \equiv (LC)^{-1/2} \approx \omega_0$. The microwave resonator was tuned to a frequency ω' close to the EPR frequency $\omega_e \approx 30$ GHz. When $\omega' < \omega_e$, the dynamic nuclear polarization has a negative sign, i.e., a raser is realized. The voltage in the circuit was measured, which is proportional to the total magnetic field in the coil containing the specimen.

The dynamics of the nuclear magnetization is described by the Bloch equations, which have the following form in a system of coordinates rotating at the frequency $\omega = \omega_0$:

$$\dot{\mu}_+ = -\Gamma_2 \mu_+ + i\gamma H_+ \mu_z,$$
$$\dot{\mu}_z = -\Gamma_1(\mu_z - \mu_e) + \frac{i}{2}\gamma(\mu_+ H_- - \text{c.c.}). \tag{4.1}$$

Here μ_e is the nuclear magnetization arising from the dynamic polarization of the nuclear spins, $H_+ = H_x + iH_y$, γ is the gyromagnetic ratio for the nuclei, and we have $\Gamma_{1,2} = T_{1,2}^{-1}$ ($T_{1,2}$ are the times of longitudinal and transverse nuclear relaxation). To find the alternating magnetic field in the coil, one can use the ordinary equations of an LC circuit. If we assume that the transient processes in the circuit decay in a time small in comparison with the characteristic times in the nuclear system (the approximation of a low-Q-factor circuit), we obtain: $H_x = -4\pi\xi Q\mu_y$, ξ is the duty factor of the coil, and Q is the Q-factor. Upon substituting this expression into (4.1) and neglecting the nonresonance terms, we obtain equations that describe the spin dynamics with allowance for the resonator:

$$\dot{\mu}_x = -\Gamma_2 \mu_x - G\mu_x \mu_z,$$
$$\dot{\mu}_y = -\Gamma_2 \mu_y - G\mu_y \mu_z, \tag{4.2}$$
$$\dot{\mu}_z = -\Gamma_1(\mu_z - \mu_e) + G(\mu_x^2 + \mu_y^2).$$

Here we have $G = 2\pi\gamma\xi Q$. This system has the following stationary points (it was assumed that $\mu_x \equiv 0$ and $\mu_e < 0$):

$$1)\ \mu_y = 0,\ \mu_z = \mu_e,$$
$$2)\ \mu_y = [-\Gamma_1(\Gamma_2 + G\mu_e)]^{1/2}/G,\ \mu_z = -\Gamma_2/G. \tag{4.3}$$

The former solution corresponds to the absence of emission, while the latter describes a steady-state generation regime, which is realized when $G|\mu_e| > \Gamma_2$.

To excite chaos in the raser, a weak inhomogeneous magnetic field was applied to the specimen, which increases the width of the NMR line. This field varied in time according to a sinusoidal law with a frequency f close to the frequency of the linear oscillations near the stationary point of (4.3) ($f \sim 50 - \sim 100$ Hz). One can take account of the influence of this field in the equations of motion (4.2) by making the substitution $\Gamma_2 \to \Gamma_2(1 + \Lambda \sin 2\pi f t)$. The thermal noise in the raser was modeled by an extra field that was introduced into Eqs. (4.2) as an adjustment parameter ($\sim 10^{-6}$ Oe). Here qualitative agreement was observed between the results of numerical calculation with the described model and the actual experiment. It turned out that chaos arises already at a very small amplitude of modulation $\Lambda \sim 10^{-3}$. Here transition to chaos was observed via doubling bifurcations of the period $T \equiv f^{-1}$. Upon varying the frequency f and the amplitude Λ, a transition to chaos was also observed via alternation, the coexistence of different attractors, and hysteresis.

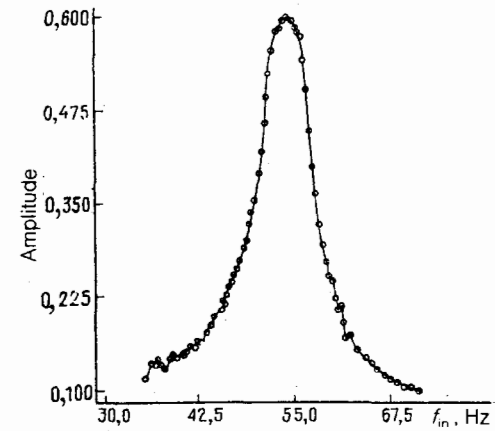

FIG. 14. Observed response of an NMR maser in the case of parametric pumping with $f = 110$ Hz as a function of the frequency of the weak signal f_{in}.[46]

As is known, near a doubling bifurcation point a nonlinear system is very sensitive to external agents. In principle this enables one to use it as a detector or amplifier.[45] In Ref. 46 a raser existing near a doubling bifurcation point was used as a detector of weak signals. The situation was studied in detail in which the period-doubling bifurcations arise from Q-switching of the raser. Moreover, a weak inhomogeneous magnetic field was applied to the specimen with the frequency $(f/2) + \delta$, which altered the width of the NMR line. This modulation played the role of the weak signal. As $\delta \to 0$, the amplitude of the beats at the output of the raser increased (Fig. 14). As we see from this diagram, the dependence of the response on δ has a sharply marked resonance character. Analogous results were observed near the bifurcation point $2T \to 4T$. By using a raser model of the type of (4.2), it was shown numerically in Ref. 46 that the sensitivity of such a detector increases as the value of the control parameter r approaches the doubling bifurcation point r_c as $|r - r_c|^{-1.5}$. The authors of Ref. 46 consider that such detectors of weak signals based on unstable maser systems can operate in the range $1 - 10^6$ Hz.

5. HAMILTONIAN CHAOS IN SPIN SYSTEMS

The study of Hamiltonian chaos in spin systems began in the mid-eighties, and by now results have been obtained on the dynamics of classical conservative[47–53] and nonautonomous[54–59] systems.[9)] We must note immediately that all these studies are theoretical, and at present we know of no experiments to observe Hamiltonian chaos in spin (magnetic) systems.

5.1. Conservative systems

One of the simplest physical models that allows Hamiltonian chaos is a system of two classical spins having the Hamiltonian[48]

$$H = \sum_{\alpha=x,y,z} \{-J_\alpha S_1^\alpha S_2^\alpha + \frac{1}{2}A_\alpha[(S_1^\alpha)^2 + (S_2^\alpha)^2]\}, \tag{5.1}$$

which takes account of the exchange interaction and single-

ion anisotropy. It was shown analytically[48] that this system has a second (independent of H) integral of motion that is quadratic in the spin variables only if the condition is satisfied that

$$(A_x - A_y)(A_y - A_z)(A_z - A_x) + \sum_{\alpha\beta\gamma=\mathrm{cycl}(x,y,z)} J_\alpha^2(A_\beta - A_\gamma) = 0. \tag{5.2}$$

It was shown numerically[48,50] that breakdown of the condition (5.2) leads to the absence, not only of quadratic, but also of any other integral independent of H. Here the motion of the spins is chaotic under most initial conditions (global chaos). An example of a system of (5.1) with breakdown of the condition (5.2) is the Hamiltonian of an XY-model with single-node anisotropy:

$$H_\alpha = -(S_1^x S_2^x + S_1^y S_2^y) - [(S_1^x)^2 + (S_2^x)^2 - (S_1^y)^2 - (S_2^y)^2]/2. \tag{5.3}$$

This model is fully integrable only when $\alpha = 0, \pm 1$. The dynamical properties of the models of (5.1) and (5.3) (behavior of the autocorrelation functions and the analytic properties of the time averages) were studied in Ref. 49. Chaos in three-spin chains was studied in Refs. 51 and 52, while certain generalizations to a larger number of spins are contained in Ref. 50.

It was shown in Ref. 53 that a transition to chaos can occur even in the very simple case of free, homogeneous oscillations of the magnetization in an antiferromagnet. An easy-axis, two-sublattice antiferromagnet was studied that was situated in a constant magnetic field inclined with respect to the axis of anisotropy. To describe the dynamics of the magnetization of each sublattice, the dissipation-free Landau–Lifshits equations were used. Here the system is reduced to a Hamiltonian system with two degrees of freedom, which is nonintegrable and allows a chaotic dynamics. It is interesting to note that the analogous homogeneous oscillations of the magnetization in a ferromagnet are regular, since this system has only one degree of freedom and is fully integrable.

5.2. Nonautonomous systems. Chaos in nonlinear NMR

This section is devoted to studying the chaotic dynamics of a spin on which an alternating magnetic field is acting.[54–59] Here we shall discuss in greater detail the problem of the transition to chaos in nonlinear NMR with a dynamic frequency shift (DFS) of precession.[56–59] At present NMR with a DFS is apparently the most probable system in which one can experimentally observe magnetic Hamiltonian chaos.[10)]

A DFS proportional to the longitudinal component of the nuclear magnetization is one of the simplest and comparatively well studied types of nonlinear NMR.[60–62] The appearance of a DFS of NMR involves the electronic-nuclear hyperfine interaction and is observed in magnetically ordered materials (ferromagnets and antiferromagnets) at liquid-helium or lower temperatures.

The possibility of onset of chaos in NMR with a DFS was first demonstrated in Refs. 56 and 57. Here we shall present this problem, following Ref. 58.

Let us choose the coordinate system as follows: we shall direct the z axis along the magnetic field $\mathbf{H}$ that acts on the nuclear spins (the field $\mathbf{H}$ amounts to the sum of the external constant field and the internal hyperfine $\mathbf{H}_n$ created by the magnetic moments of the electrons on the nuclei), while the x axis of the rotating system of coordinates is directed antiparallel to the external alternating field $H_+ = H_1(t)\exp(-i\omega t)$. Then the equations of motion in the rotating system of coordinates have the form[60–62]

$$\begin{aligned} \dot{u} &= v(\Delta - \omega_p m), \\ \dot{v} &= -u(\Delta - \omega_p m) + \omega_1(t) m, \\ \dot{m} &= -\omega_1(t) v, \\ u^2 + v^2 + m^2 &= 1, \end{aligned} \tag{5.4}$$

Here we have $\Delta = \omega_n - \omega$, $\omega_n = \gamma(H_n - H_0)$ is the NMR frequency without taking account of the DFS (γ is the gyromagnetic ratio for the nucleus), ω_p is the nonlinearity parameter ($\omega_p \ll \omega$), which amounts to the maximum DFS at the equilibrium value of the magnetization, $\omega_1(t) = \gamma A \chi H_1(t)$, A is the dimensionless hyperfine-interaction constant, and χ is the transverse static susceptibility of the electronic magnetic subsystem. The variables u, v, and m are the components of the nuclear-magnetization vector (normalized to the equilibrium value of the magnetization) in the rotating system of coordinates. The equations (5.4) are valid if one neglects the effects of irreversible relaxation and inhomogeneous broadening of the NMR line. Let the envelope of the alternating magnetic field acting on the nuclear spins be fixed in the form of a periodic sequence of short pulses of area α and period of repetition T. Such a formulation of the problem arises in studying various transition phenomena in NMR: decay of the free induction, spin echo, etc.[61,62] Moreover, this enables one to reduce the system of equations (5.4) to a mapping that associates the values of the components of the nuclear magnetization before the nth and $(n+1)$th pulses. This area-conserving mapping amounts to a combination of two rotations: in the $v - m$ plane by the angle α (equal to the area of the pulse), and in the $u - v$ plane by the angle ϕ_n, which depends on the values of m_n and v_n: $\varphi_n = \Delta T - \omega_p T(m_n \cos\alpha - v_n \sin\alpha)$. We note that, when $\alpha \ll 1$ and under the initial condition $m_0 \approx 0$, this mapping is reduced to the standard mapping (see Sec. 2). Using the criterion of overlap of nonlinear resonances or the criterion of phase extension, we can derive the following condition for strong chaos:

$$K = \omega_p T \sin^2\alpha \gg 1. \tag{5.5}$$

It is important to note that (5.5) can be satisfied under the natural initial conditions $m_0 = 1$, $u_0 = v_0 = 0$ (the ground state). An interesting feature of the given system is the existence of windows of regularity. For example, when $\alpha = \pi/2$, the centers of the windows are determined by the equations $\omega_p T = l\pi$ (l = integer, $m_0 = 1$), while their width is $\sim 1/K$. The windows of regularity are highly typical of dissipative systems, whereas only a few examples are known for Hamiltonian systems.[63] Thus, in NMR with a DFS several transitions of the type order-chaos-order can occur as one varies the area of the exciting pulses α or the dimensionless nonlinearity $\omega_p T$.

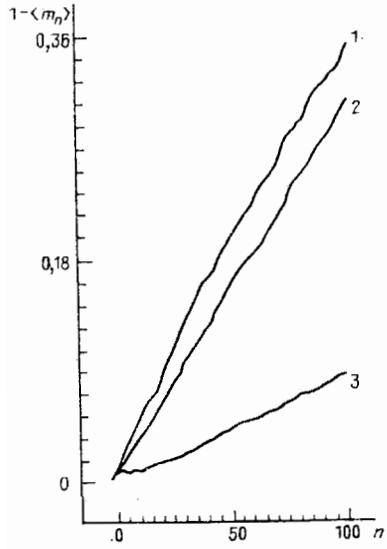

FIG. 15. Stochastic excitation of nuclear magnetization. $m(0) = 1$; $\alpha = 0.1$; $\omega_p T = 628$ (*1*), 314 (*2*), and 90 (*3*). (Ref. 58).

In most experimental situations inhomogeneous broadening exerts a substantial influence on NMR with DFS.[62,64] As is known, the main physical cause of inhomogeneous broadening is inhomogeneity of the susceptibility χ, which leads to a scatter of values of the DFS parameter ω_p.[64] The manifestations of chaotic motion of the magnetization upon taking account of the influence of inhomogeneous broadening differ for $\alpha \ll 1$ and for $\alpha \sim \pi/2$.

1) *Small pulse area* $\alpha \ll 1$. In chaos the mean value of the longitudinal component of the magnetization $\langle m \rangle$ deviates from the equilibrium value $m_0 = 1$–stochastic excitation (Fig. 15).[56,58] The symbol $\langle ... \rangle$ here denotes averaging that takes account of the inhomogeneous broadening, which in this case plays the role of averaging over the ensemble (see Sec. 2). Such a strong deviation of the transverse component of the magnetization is impossible in nonlinear regular motion.

2) *Let* $\alpha \sim \pi/2$ *and* $T/T_2^* \ll 1$ (T_2^* is the characteristic time of inhomogeneous relaxation). In this case the decay of the mean values of the transverse $\langle m_\perp \rangle$ and longitudinal $\langle m \rangle$ components of the magnetization occurs considerably faster in chaotic dynamics than in regular dynamics. This effect is shown in Fig. 16, where close-lying values of the nonlinearity $\omega_p T$ correspond to a window of regularity (dashed curve) and chaos (solid curve). The reason for such behavior is the rapid (see (2.10)) splitting of the correlations of the motion of individual isochromats in chaos, which leads to self-averaging of the quantities $\langle m_\perp \rangle$ and $\langle m \rangle$.

A suitable object for observing chaos in NMR is apparently an antiferromagnet at liquid-helium temperatures with relaxation times $T_2 \sim 10^{-4} - 10^{-3}$ s and $T_1 \sim 10^{-3} - 10^{-1}$ s and with a sufficiently strong DFS $\omega_p \sim 10^5 - 10^7$ Hz. To observe stochastic excitation one can propose the following experimental scheme: after N short pulses ($N \sim 5$–10), one applies another pulse after a time τ ($T_2 < \tau < T_1$) and observes the free-induction signal. The amplitude of this signal depends on the magnitude of the longitudinal component of the magnetization, while in turn it differs for regular and chaotic dynamics under the action of the N pulses.

In Ref. 59 the possibility of chaotization of the motion of the magnetization in NMR with a DFS was studied upon applying two external alternating fields: a longitudinal resonance field with constant amplitude (H_1 = const in (5.4)) and a weak transverse field with frequency $\nu < \omega_p$. As had been shown earlier,[60] when ω_1 = const in the system of (5.4), an aperiodic trajectory exists with a period of motion $\to \infty$, which corresponds to the separatrix in the phase portrait. On applying a weak longitudinal field in the neighborhood of the separatrix, a stochastic layer arises, whose width depends on the amplitude and frequency of this field. This stochastic layer can include the ground state of the magnetization if $\Delta = 0$ and $\omega_1 = \omega_p$. Here the motion of the magnetization is random.

6. QUANTUM CHAOS IN SPIN SYSTEMS

In the previous sections of the review, we have used everywhere the classical or semiclassical approach in describing chaotic dynamics in spin systems. As a rule, such an approach is adequate, but nevertheless, the spin is a purely quantum object, and therefore a consistent description of nonlinear spin dynamics requires a completely quantum treatment. Thus, we arrive at the formulation of the problem of quantum chaos in spin systems: what are the features of

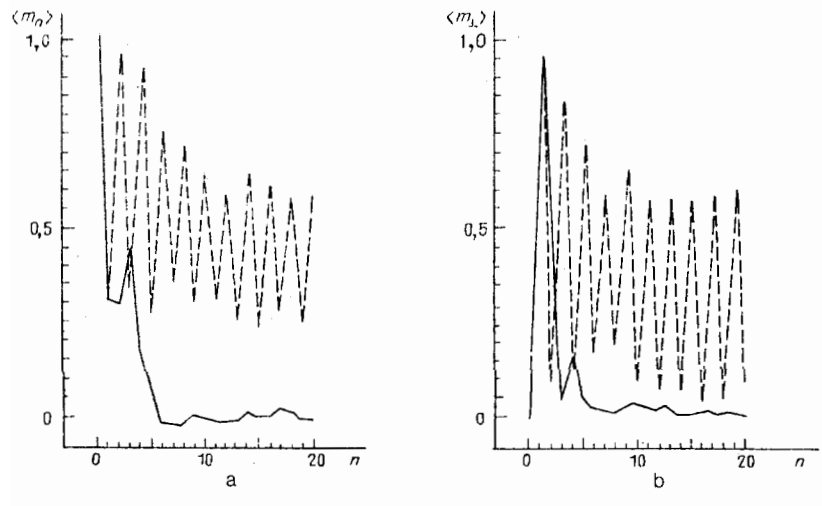

FIG. 16. Nonlinear dynamics of the averages of the longitudinal (a) and transverse (b) components of nuclear magnetization for values of the parameters corresponding to chaos (solid curve) and a window of regularity (dashed).[58]

the dynamics and the properties of stationary states of quantum spin systems that possess a chaotic dynamics in the classical limit ($S \to \infty$)?[11)]

We do not have here the possibility of describing in any detail the results of the studies on quantum chaos in various physical systems, but refer the reader to the reviews on this problem (Refs. 5, 7, 8, 66–68).

Most of the studies on quantum chaos have been performed using examples of several models, the most popular of which are: a rotator excited with a periodic sequence of δ-pulses (Refs. 5, 7, 8, 66–69) (the quantum analog of the standard mapping of (2.3)), and nonlinear oscillators (Refs. 5, 7, 8, 66–68, 70). We note also that almost all current studies on quantum chaos deal with Hamiltonian systems; the study of dissipative quantum systems that possess a chaotic dynamics in the classical limit is only beginning (see, e.g., Ref. 71 and the references cited there).

The study of quantum chaos in spin systems began in the eighties, and the currently existing studies are relatively few (at least in comparison with the total number of studies on quantum chaos) (Refs. 51, 52, 54, 72–79, 86). We should note immediately that all these studies are theoretical, and that most of them present the results of numerical experiments. This situation results from the newness of this field, together with the complications that arise here of theoretical and experimental study.

In studying quantum chaos in spin systems only several simple models of conservative and nonautonomous systems have been treated:

1) *The model of coupled rotators*[72] (the classical dynamics was studied in Ref. 47):

$$H = A(L^z + M^z) + BL^xM^x, \tag{6.1}$$

Here A and B are constants, while the variables L and M have commutation relationships for the angular-momentum operators. There are three integrals of the motion: H, $\mathbf{L}^2$, and $\mathbf{M}^2$. Although the Hamiltonian in (6.1) apparently does not describe any real physical system,[12)] it has a structure typical of spin Hamiltonians. A study of a classical system with the Hamiltonian function of (6.1) showed[47] that it is nonintegrable and admits global chaos at an energy greater than a certain critical value, and with fixed $\mathbf{L}^2$ and M^2.

2) *A chain of spins with periodic boundary conditions, antiferromagnetic exchange interaction, and anisotropy*:[51,52,73]

$$H = J\sum_{i=1}^{3}(\mathbf{S}_i\mathbf{S}_{i+1} + \sigma S_i^zS_{i+1}^z),\ \mathbf{S}_4 = \mathbf{S}_1. \tag{6.2}$$

Here we have $J > 0$, $-1 \leqslant \sigma \leqslant 0$. When $\sigma \neq 0$ there are two integrals of motion: H and $T^z = \Sigma_{i=1}^3 S_j^z$, while when $\sigma = 0$ the system of (6.1) is fully integrable (in this case, besides H and T^z, there are three additional integrals of motion–the components of $T = \Sigma_{i=1}^3 S_j$.[50,51,73] The classical treatment ($S \to \infty$) of the model of (6.2) shows[50,51] that, when T^z is fixed ($T^z = 0$) and $J = 1$, an increase in the parameter of nonintegrability $|\sigma|$ leads to global chaos over a rather broad interval of energies. The authors of Refs. 51 and 52 consider that a Hamiltonian of the form of (6.2) can describe spin clusters of Fe^{2+} ions in an antiferromagnet having the trigonal lattice of $RbFeCl_3$.

3) *Nonautonomous models describing a spin on which an external periodic field $B(t)$ is acting, with account taken of anisotropy*:

$$H = \mu H_0(\mathbf{S}) + \varepsilon F(\mathbf{S})B(t). \tag{6.3}$$

Here μ and ε are parameters, while the functions $H_0(\mathbf{S})$, $F(\mathbf{S})$, and $B(t)$ have the form

$$H_0(\mathbf{S}) = (S^z)^2,\ F(\mathbf{S}) = \mathbf{S},\ B(t) = B_x = \cos\omega t \text{ (see Ref. 54)}, \tag{6.4}$$

$$H_0(\mathbf{S}) = (S^z)^2,\ F(\mathbf{S}) = S^x,\ B(t) = \delta_T(t) \text{ (see Refs. 74–76)}, \tag{6.5}$$

$$H_0(\mathbf{S}) = S^y,\ F(\mathbf{S}) = (S^z)^2,\ B(t) = \delta_T(t) \text{ (see Refs. 54, 77)}. \tag{6.6}$$

Hamiltonians are also studied in which H_0 and F are more complex polynomials of the components of the spin $\mathbf{S}$.[77–79]

Now let us examine the fundamental features of quantum chaos in the spin systems of (6.1)–(6.3).

6.1. Dynamics of the observables

Since the energy spectrum of the systems being discussed is discrete, and moreover, finite, the dynamics of the observable quantities is always regular and quasiperiodic. However, according to the correspondence principle, in the quasiclassical region ($S \gg 1$), features of classical chaos must be manifested. Therefore the first question of interest is the following: In the course of what time will a quantum spin system with $S \gg 1$ manifest the properties of a classical chaotic system? The answer to this question, with the example of the models of (6.3), (6.4), and (6.6), is found in Refs. 54 and 55–the time of applicability of the classical description for a quantum chaotic system is

$$\tau_{cl} \sim (1/\lambda)\ln S, \tag{6.7}$$

Here λ is the value of the Lyapunov exponent of the classical system, while the time τ is measured in units of the characteristic frequency ω in the system: $\tau = \omega t$. When $\tau > \tau_{cl}$, the dynamics of the observables differs strongly from the dynamics of the corresponding classical quantities. To understand this result, we shall present, following Ref. 55, some simple qualitative arguments. The minimal phase uncertainty for the spin S is $\Delta\varphi \sim S^{-1/2}$. In the course of time this uncertainty will increase according to the law $\Delta\varphi(\tau) \sim \Delta\varphi(0)\exp(\lambda\tau)$, while the characteristic time τ at which the phase uncertainty reaches $\Delta\varphi \sim 1$ is $\tau_{cl} \sim \lambda^{-1}\ln S$.

One can show[54,55] that for spin systems with a regular dynamics the corresponding time of applicability of the classical description is

$$\tau_{cl} \sim S^{\alpha},\ \alpha = \text{const} \sim 1. \tag{6.8}$$

If we take account of the fact that $S \propto \hbar^{-1}$, then the estimate (6.7) agrees well with the analogous estimate obtained earlier for a nonlinear oscillator:[70] $\tau_{cl} \propto \ln\hbar^{-1}$. The time in (6.7) is rather short. For example, in the numerical experiment of Ref. 55, τ_{cl} amounts to only ≈ 8 iterations for $S = 100$.

Now let us discuss how the dynamics of the observables at times $\tau > \tau_{cl}$ differs in cases when the spin dynamics is

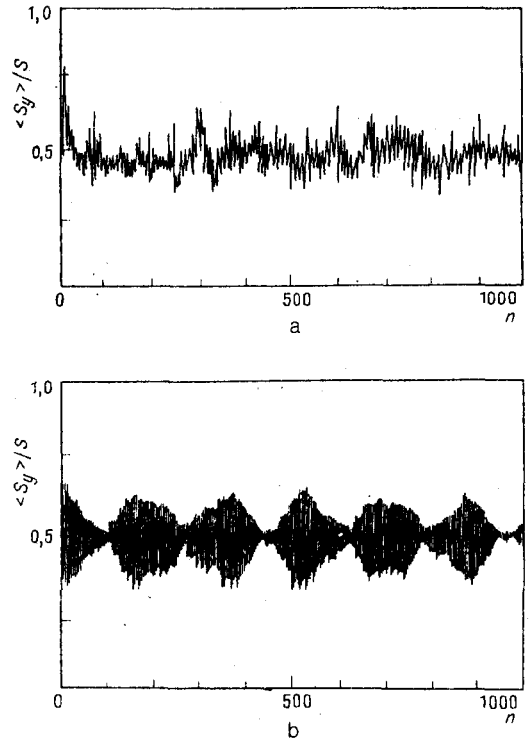

FIG. 17. Dynamics of the quantum averages ($S = 100$) for regular (a) motion in the classical limit (b) and chaotic.[55]

regular or chaotic in the classical limit. In both cases the dynamics of the averages is quasiperiodic. However, while in the regular regime (Fig. 17a) this is a periodic sequence of collapses and regeneration of oscillations with the characteristic quasiperiod S, in the chaotic regime (Fig. 17b) it amounts to complex oscillations in which it is hard to distinguish the characteristic period. Correspondingly also the number of functions $N_{\min}$ of the evolution operator $U(t) = \exp(i/\hbar H)$ that effectively contribute to the dynamics of the averages (the observables) differs substantially. In the regular regime we find $N_{\min} \lesssim 10$, while in the chaotic regime $N_{\min} \sim 10^2$ when $S = 100$ (Ref. 55). Thus, besides the quasiclassicity $S \gg 1$, another condition for observing quantum chaos is the involvement in the dynamics of a large number of levels.

One of the interesting manifestations of quantum effects in chaos, which has been best studied for the model of a quantum rotator, is the effect of quantum restriction of diffusion (QRD).[8,69] In a rotator the effect of QRD consists in the saturation at characteristic times t_D of the diffusional increase in the quantity $\langle p^2 \rangle$ (p is the momentum) or the energy of the system.[8,69] QRD has deep analogies in the effect known in the physics of disordered states of Anderson localization in a random potential.[80] At present QRD is the main one of the effects predicted by the theory of quantum chaos that is verified in experiments with hydrogen atoms.[81] An interesting feature of spin systems with quantum chaos is the absence in the general case of localization in terms of the angular momentum.[76] This involves the differing topology of the phase space: for a rotator it is a cylinder not bounded in momentum, while for a spin system it is a sphere. However, in certain special cases QRD (localization) is possible also for spin systems. Thus, for example, for the models of (6.3) and (6.5) in the case in which the initial conditions have been chosen near the equator $S^z \ll S$ and $\mu \to \infty$, $\varepsilon \to 0$, the top of (6.3) goes over into a rotator and localization in the variable S^z can occur.[76]

6.2. Energy spectrum and wave functions

Substantial differences in the behavior of regular and chaotic spin systems are manifested in their energy spectrum and in the structure of the eigenfunctions. In the case of nonautonomous systems with a periodic perturbation, one studies the spectrum of quasienergies and quasienergy eigenfunctions.[82]

In chaos the spectrum is unstable with respect to small changes of the parameters of the system.[83] Thus, for the model of (6.2) the quantities

$$\chi = \left\langle\left\langle \frac{\Delta^2 E}{\Delta\sigma^2} \right\rangle\right\rangle = \left\langle\left\langle \frac{E(\sigma + \Delta\sigma) - 2E(\sigma) + E(\sigma - \Delta\sigma)}{(\Delta\sigma)^2} \right\rangle\right\rangle, \quad (6.9)$$

$$\langle\langle(\Delta\chi)^2\rangle\rangle = \left\langle\left\langle \left[\frac{\Delta^2 E}{\Delta\sigma^2} - \left\langle\left\langle \frac{\Delta^2 E}{\Delta\sigma^2} \right\rangle\right\rangle \right]^2 \right\rangle\right\rangle, \; S \gg 1 \quad (6.10)$$

($\langle\langle ... \rangle\rangle$ denotes averaging over a certain interval of energies) increase with increasing S in chaos and actually do not depend on S in regular motion.[51,52] When $\sigma = 0$ (integrable limit), the absolute magnitude of (6.9) and (6.10) was approximately of the same order as when $\sigma \neq 0$ throughout the energy ranges. Therefore the authors of Refs. 51 and 52 assume that the characteristics of the instability of the spectrum in chaos must be not the absolute values of the "susceptibilities" χ of (6.9) and their variance of (6.10), but their dependence on the quasiclassicity parameter S. To characterize this dependence quantitatively, the following quantity was introduced in Refs. 51 and 52:

$$g(S) = \frac{[\langle\langle(\Delta\chi)^2\rangle\rangle]^{1/2}}{|\chi|} \quad (6.11)$$

and the existence of a scaling $g(S)$ was shown numerically:

$$g(\Lambda S)/g(S) = \Lambda^{\beta(\sigma)}, \; S \gg 1. \quad (6.12)$$

We find that the exponent $\beta(\sigma) > 0$ for the regions in the parameter σ and in the energy that correspond to classical chaos; $\beta(\sigma) \leqslant 0$ for regular motion.

The transition to quantum chaos is characterized not only by the appearance of a fractal structure of the energy spectrum in (6.12), but also by the appearance of a fractal structure of the eigenfunctions for conservative and nonautonomous systems.[73,74]

In Ref. 73, using the example of the model of (6.2), the fine structure and scaling properties of the eigenfunctions were studied in the Fock representation and in the classical limit ($S = 16 - 32$). The following procedure of scale coarsening of the eigenfunctions $\psi(m_1, m_2)$ was defined:[13)] for a given linear dimension ε, a cell was studied $A(\varepsilon) = \varepsilon \times \varepsilon$ in the neighborhood of the given $m_{1,2}$, and then the measure $\mu(\varepsilon)$ of the regions satisfying the following condition was calculated:

$$\left[\frac{\varepsilon_0}{\varepsilon}\right]^2 \sum_{m_{1,2} \in A(\varepsilon)} \psi(m_1, m_2) \geq C, \quad (6.13)$$

Here C is a constant, while $\varepsilon_0 \sim S^{-1}$ is the smallest possible scale of resolution of the structure of the eigenfunctions. In studying the dependence of the measure $\mu(\varepsilon)$ on ε, as ε decreases down to $\varepsilon = \varepsilon_0$, the following scaling relationship was obtained:

$$\mu(\varepsilon) = \mu(0) + k\varepsilon^{\beta}, \quad k = \text{const} > 0, \tag{6.14}$$

Here we have $\beta \geqslant 1$ for regular motion and $\beta < 1$ for chaos. Such a scaling ($\mu(0) \neq 0$) is characteristic of the so-called fat fractals.[84] The relationship (6.14) shows the difference of the eigenfunctions in the regular and chaotic regimes of motion: a regular structure of the eigenfunctions leads to a rather smooth dependence of μ on ε for small ε ($\beta \geqslant 1$), while irregularity of the eigenfunctions leads to the situation in which its fine structure can be distinguished only on small scales $\varepsilon \sim \varepsilon_0$.[73]

In Ref. 74 the fractal structure of the eigenfunctions was studied for the nonautonomous model of (6.3) and (6.5). It was shown that the perimeter of the contour L of a coarsened quasienergy eigenfunction admits the following scaling:

$$L \propto \varepsilon^{D}, \tag{6.15}$$

Here $\varepsilon \geqslant \varepsilon_0$ is the scale of the coarsening; $\varepsilon_0 \sim S^{-1}, S = 128$; the coarsening procedure is essentially analogous to (6.13). We find that the exponent $D = 1$ in the integrable limit, whereas in chaos $D > 1$, and increases with increasing degree of chaoticity, reflecting the structure of the eigenfunction, which becomes more complicated.

Thus the spectrum and the structure of the eigenfunctions of spin systems in quantum chaos possess fractal properties. As is known, fractality is an intermediate quality between complete randomness and complete determinacy. Therefore the appearance of fractal properties in quantum chaos apparently involves the fact that quantum chaos ($S \gg 1$) is an intermediate quality between the complete determinacy (in the dynamical sense) of quantum dynamics ($S < 1$) and chaos in the classical limit ($S \to \infty$).

The irregular structure of the eigenvalues and the eigenfunctions in spin systems in quantum chaos is also manifested in the behavior of the propagator (Green's function) and the structure of the matrix elements of the operators, which do not commute with the Hamiltonian[72] (studies using the example of the model of (6.1).

Since the spectrum and structure of the eigenfunctions of quantum chaotic systems are highly complex, it is natural to describe them statistically. As a result of many numerical experiments devoted to studying the statistics of systems with quantum chaos, a connection has been established with the theory of random matrices, which studies the statistics of eigenvalues and eigenfunctions of ensembles of matrices with random elements.[85] The statistical properties of these ensembles are invariant with respect to transformation groups that preserve the symmetry of the original Hamiltonian. In the theory of random matrices one distinguishes three types of similar transformations: orthogonal, unitary, and symplectic. Correspondingly the statistical properties of the eigenvalues and the eigenvectors of the matrices are distinguished.

One of the most popular statistical characteristics of a spectrum is the distribution function of distances between neighboring levels $P(\Delta E)$. Numerical experiments with spin systems in the quasiclassical region $S \gg 1$ showed[55,75,77–79] that in the case of global quasiperiodicity the $P(\Delta E)$ distributions have a form close to a Poisson distribution $P(\Delta E) \propto \exp(-\Delta E)$ ($P(\Delta E \to 0) \neq 0$), while in the case of global chaos $P(\Delta E)$ has a substantially different form, with $P(\Delta E \to 0) \propto \Delta E^{\alpha}$, $\alpha = \text{const}$. The latter property involves the repulsion of levels in a regime of quantum chaos, while the degree of repulsion α depends on the symmetry properties of the original Hamiltonian:

a) *If the Hamiltonian is invariant with respect to time-reversal operations, then $\alpha \approx 1$.* In the theory of random matrices this corresponds to the so-called Gaussian ensemble of real symmetric matrices, which is invariant with respect to orthogonal transformations. Examples of such a system are the models (6.3), (6.6)[55,77] and (6.3), (6.5).[75]

b) *Breakdown of T-invariance leads to quadratic repulsion of levels: $\alpha \approx 2$.* (Refs. 55, 77). An example is a system defined by the evolution operator after one impulse:

$$U = \exp(-ik'S_x^2)\exp(ikS_z^2)\exp(-ipS_y), \quad p \neq \frac{\pi}{2}, \quad k \neq k'. \tag{6.16}$$

The contrast of (6.16) with the system of (6.3) and (6.6) consists in the presence of an additional perturbation that leads to rotation about the x axis. In the theory of random matrices this case corresponds to the so-called Gaussian unitary ensemble, whose statistical properties are invariant under unitary transformations.

c) *There are also spin systems with quantum chaos that correspond to symplectic ensembles of random matrices and which allow repulsion with $\alpha \approx 4$.* An example is a Hamiltonian of the form of (6.3), in which we have[77,79]

$$H_0 = S_z^2, \quad F = S_z^2 + k_1(S_xS_z + S_zS_x) + k_2(S_xS_y + S_yS_x), \quad B(t) = \delta_T(t). \tag{6.17}$$

The statistics of the eigenfunctions of chaotic spin systems agrees well with the statistics of the eigenvalues, which corresponds to one of the types of ensembles of random matrices.[77]

We must note that the agreement between the statistics of the spectrum of chaotic systems and the statistics of the spectrum of random matrices operates only in the quasiclassical limit $S \gg 1$. Here this agreement is not complete, even when $S \sim 10^2$—study of the subtler statistical characteristics shows the presence of quantitative discrepancies between the predictions of the theory of random matrices and the results of numerical study of Hamiltonians with quantum chaos.[75] Moreover, we must note that chaotic systems in which the islands of stability in the classical limit occupy an appreciable fraction of phase space demonstrate certain intermediate statistics, i.e., statistics that is neither Poisson nor statistics corresponding to any type of ensembles of random matrices.

A recent study[86] investigated the statistics of the spectrum of spin systems of the type of (6.3) with account taken of dissipation. It was shown numerically that, if the corresponding classical system possesses a regular dynamics, the repulsion of levels is linear, $\alpha \approx 1$, while if it is chaotic, then the repulsion is cubic, $\alpha \approx 3$. In the case of chaos the degree

of repulsion apparently does not depend on the symmetry of the generating Hamiltonian.

6.3. Discussion

Thus, in order to be able to observe the phenomenon of quantum chaos in a spin system, the following fundamental conditions must be satisfied: a) quasiclassicity ($S \gg 1$), b) many levels must participate in the dynamics of the system; c) a sufficiently developed chaos must exist in the corresponding classical system (as $S \to \infty$).

The fundamental manifestations of quantum chaos include: the appearance of a complex (fractal) structure of the eigenfunctions and of the spectrum; and change of the statistics of the spectrum on going from regular to chaotic behavior. The energy spectrum of systems that possess developed chaos in the classical limit is characterized by several universal statistics that depend on the symmetry properties of the Hamiltonian.

We must note that, in comparison with other systems, spin models possess an important advantage connected with the finiteness of their spectrum. In the numerical study of systems with an unbounded spectrum, one must always introduce an artificial procedure of spectrum cutoff, which can alter the latent symmetry of the system and thus lead to false physical results. In this sense the models of spin systems are an ideal object for studying problems of quantum chaos.

As we have already noted, at present experiments on quantum chaos in spin systems are lacking. This apparently involves in many ways the insufficient knowledge of the new fundamental results obtained in the theoretical study of the phenomenon of quantum chaos in recent years.[14)] As we see it, such systems are a quite good object for studying quantum chaos, since, first, in many typical experiments spin systems are quasiclassical, and second, a sufficient experience has already been accumulated in the chaotic dynamics in magnetic systems. Apparently, above all of greatest interest would be the experimental discovery of a change in the statistics of the spectrum in an order-chaos transition and observation of the correspondence time τ_{cl} of (6.7).

The progress in the experimental study of quantum chaos in spin systems is to some extent hindered also by the fact that all the theoretical results were obtained for few-particle systems, while almost all real spin (magnetic) systems are multiparticle. However, at present the theory of quantum chaos in multiparticle systems has not been developed.

Thus the study of quantum chaos in magnetic systems seems quite promising, and in the next few years here we can apparently expect new fundamental results.

We thank M. I. Rabinovich for valuable remarks.

[1)] The connection between instability of motion and the appearance of randomness had been pointed out already in the works of Poincaré.[10]

[2)] Local instability is taken to mean the exponentially rapid divergence in phase space of two trajectories close-lying at the initial instant of time. The exponent in this exponential averaged over the entire trajectory is called the maximal Lyapunov exponent. In chaotic motion the maximal Lyapunov exponent is positive for a continuous system, or greater than unity for a mapping.[5-7]

[3)] In certain cases the problem of motion of a classical spin in an alternating magnetic field is reduced to the standard mapping (see Ref. 74 and Sec. 5.2).

[4)] The condition of phase dilation $|\delta\theta_n/\delta\theta_{n-1}| > 1$ is often applied[5] as a semiqualitative criterion of strong chaos in Hamiltonian and dissipative (see (2.14)) systems.

[5)] The point x^* is called the stationary point of the mapping $f(x)$ if $x^* = f(x^*)$.

[6)] Unfortunately, in most contemporary studies on chaos in the parametric excitation of spin waves, references are lacking to the pioneering study, Ref. 22.

[7)] This problem is closely allied with the problem of studying chaos in NMR-masers (see Sec. 4).

[8)] "Oblique pumping" denotes the intermediate case between transverse and parallel pumping.

[9)] Part of these models, which are basic for studying quantum chaos, are described also in Sec. 6 of this review.

[10)] Recently Refs. 87 have been published, in which a regime of the strange-attractor type is studied in NMR with a DFS.

[11)] We note that such a formulation of the problem of quantum chaos, which is based on the correspondence principle, is the generally accepted one at present, but is not the sole formulation.[65]

[12)] In the opinion of the authors of this model, (6.1) can describe pseudospins in nuclear physics and the physics of the condensed state.

[13)] The $m_{1,2}$ are the eigenvalues of the operators $S^z_{1,2}$ in (6.2). The values of m_3 are determined from the conservation law $T^z = \Sigma^3_{j=1} S^z_j$.

[14)] We would be glad if this review facilitates to any degree the arousal of interest of experimentalists in the problem of quantum chaos in magnetic systems.

[1] G. M. Zaslavskiĭ and R. Z. Sagdeev, Introduction to Nonlinear Physics (In Russian), Nauka, M., 1988.

[2] G. Khaken, Introduction to Synergetics Springer-Verlag, N.Y., 1977 [Russ. transl., Mir, M., 1985].

[3] G. M. Zaslavskiĭ and B. V. Chirikov, Usp. Fiz. Nauk **105**, 3 (1971) [Sov. Phys. Usp. **14**, 549 (1972)].

[4] B. V. Chirikov, Phys. Rep. **52**, 263 (1979).

[5] G. M. Zaslavskiĭ, *Stochasticity of Dynamical Systems* (in Russian), Nauka, M., 1984.

[6] A. J. Lichtenberg and M. A. Lieberman, *Regular and Stochastic Motion*, Springer-Verlag, N.Y., 1983 [Russ. transl., Mir, M., 1984].

[7] H. G. Schuster, Deterministic Chaos: an Introduction Physik Verlag, Weinheim, FRG, 1984 [Russ. transl., Mir, M., 1988].

[8] B. V. Chirikov, F. M. Izrailev, and D. L. Shepelyansky, Soviet Scientific Reviews C **2**, 209 (1981).

[9] I. C. Percival, Proc. R. Soc. London A **413**, 183 (1987).

[10] H. Poincaré, *Les Méthodes Nouvelles de la Mécanique Céleste*, Paris, 1892, 1899 (Russ. transl., Selected Works, Vols. 1, 2, Nauka, M., 1971, 1972).

[11] P. W. Milonni, M.-L. Shin, and J. R. Ackerhalt, *Chaos in Laser-Matter Interactions*, World Scientific, Singapore, 1987; Phys. Rep. **28**, 205 (1985).

[12] V. E. Zakharov, S. V. Manakov, S. P. Novikov, and L. P. Pitaevskiĭ, *Theory of Solitons* (in Russian), Nauka, M., 1980.

[13] Solitons, eds. R. K. Bullough and P. J. Caudrey, Springer-Verlag, Berlin, 1980 (Russ. transl., Mir, M., 1983).

[14] B. M. Smirnov, Usp. Fiz. Nauk **149**, 177 (1986) [Sov. Phys. Usp. **29**, 481 (1986)].

[15] C. Grebogi, E. Ott, and J. A. Yorke, Science **238**, 632 (1987).

[16] M. J. Feigenbaum, J. Statist. Phys. **19**, 25 (1978); **21**, 669 (1979); Los Alamos Science **1**, 4 (1980) [Russ. transl., Usp. Fiz. Nauk **141**, 343 (1983)].

[17] Y. Pomeau and P. Manville, Commun. Math. Phys. **74**, 189 (1980).

[18] H. Suhl, Phys. Rev. Lett. **6**, 174 (1961).

[19] V. E. Zakharov, V. S. L'vov, and S. S. Starobinets, Usp. Fiz. Nauk **114**, 609 (1974) [Sov. Phys. Usp. **17**, 896 (1975)].

[20] V. S. L'vov, *Nonlinear Spin Waves* (in Russian), Nauka, M., 1987.

[21] A. M. Balk and V. E. Zakharov, Dokl. Akad. Nauk SSSR **229**, 1112 (1988) [Sov. Phys. Dokl. **33**, 270 (1988)]; A. V. Tur and V. V. Yanovskiĭ, ibid., p. 873 [Sov. Phys. Dokl. **33**, 266 (1988).

[22] E. V. Astashkina and A. S. Mikhaĭlov, Zh. Eksp. Teor. Fiz. **78**, 1636 (1980) [Sov. Phys. JETP **51**, 821 (1980)].

[23] K. Nakamura, S. Ohta, and K. Kawasaki, J. Phys. C **15**, L143 (1982); S. Ohta and K. Nakamura, *ibid.* **16**, L605 (1983).

[24] F. M. De Aguiar and S. M. Rezende, Phys. Rev. Lett. **56**, 1070 (1986).

[25] X. Y. Zang and H. Suhl, Phys. Rev. A **32**, 2530 (1985).

[26] S. M. Rezende, F. M. de Aguiar, and O. F. de Alkcantara Bonfim, J. Magn. Magn. Mater. **54–57**, 1127 (1986).

[27] S. M. Rezende, O. F. de Alkcantara Bonfim, and F. M. de Aguiar, Phys. Rev. B **33**, 5153 (1986).

[28] F. Waldner, D. R. Barberis, and H. Yamazaki, Phys. Rev. A **31**, 420 (1985); G. Broggi, P. F. Meier, R. Stoop, and R. Badii, *ibid.* **35**, 365 (1987).

[29] F. Waldner, R. Badii, D. R. Barberis, G. Broggi, W. Floeder, P. F. Meier, R. Stoop, M. Warden, and H. Yamazaki, J. Magn. Magn. Mater. **54–57**, 1135 (1986).

[30] P. H. Bryant, C. D. Jeffries, and K. Nakamura, Phys. Rev. A **38**, 4223 (1988).

[31] T. L. Gill and W. W. Zachary, J. Appl. Phys. **61**, 4130 (1987).

[32] H. Suhl and X. Y. Zang, Phys. Rev. Lett. **57**, 1480 (1986).

[33] H. Suhl and X. Y. Zang, J. Appl. Phys. **63**, 4147 (1988).
[34] G. Gibson and C. Jeffries, Phys. Rev. A **29**, 811 (1984).
[35] M. Mino and H. Yamazaki, J. Phys. Soc. Jpn. **55**, 4168 (1986).
[36] H. Yamazaki, *ibid.* **53**, 1155 (1984).
[37] H. Yamazaki and M. Warden, *ibid.* **55**, 4477 (1986).
[38] H. Yamazaki, M. Mino, H. Nagashima, and M. Warden, *ibid.* **56**, 742 (1987).
[39] T. L. Carroll, L. M. Pecora, and F. J. Rachford, Phys. Rev. Lett. **59**, 2891 (1987).
[40] A. A. Stepanov, A. I. Zvyagin, S. V. Volotskiĭ, M. I. Kobets, and V. A. Pashchenko, Fiz. Nizk. Temp **15**, 100 (1989) [Sov. J. Low Temp. Phys. **15**, 57 (1989)].
[41] A. I. Smirnov, Zh. Eksp. Teor. Fiz. **90**, 385 (1986) [Sov. Phys. JETP **63**, 222 (1986)].
[42] A. I. Smirnov, *ibid.* **94**(5), 185 (1988) [Sov. Phys. JETP **67**, 969 (1988)].
[43] E. Brun, B. Derighetti, R. Holzner, and M. Ravani, Acta Phys. Austriaca **56**, 85 (1984).
[44] D. E. Chyba, J. Opt. Soc. Am. B **5**, 916 (1988).
[45] K. Wiesenfeld and B. McNamara, Phys. Rev. Lett. **55**, 13 (1985).
[46] B. Derighetti, M. Ravani, R. Stoop, P. F. Meier, and E. Brun, *ibid.* **55**, 1746 (1985).
[47] M. Feingold and A. Peres, Physica D **9**, 433 (1983).
[48] E. Magyari, H. Thomas, R. Weber, C. Kaufman, and G. Müller, Z. Phys. B **65**, 363 (1987).
[49] Srivastava, C. Kaufman, G. Müller, E. Magyari, R. Weber, and H. Thomas, J. Appl. Phys. **61**, 4438 (1987); **63**, 4154 (1988).
[50] Srivastava, C. Kaufman, G. Müller, R. Weber, and H. Thomas, Z. Phys. B **70**, 251 (1988).
[51] K. Nakamura, Y. Nakamura, and A. R. Bishop, Phys. Rev. Lett. **54**, 861 (1985).
[52] K. Nakamura and A. R. Bishop, Phys. Rev. B **33**, 1963 (1986).
[53] V. Yu. Gonchar, N. N. Nasonov, and V. D. Tsukanov, Pis'ma Zh. Tekh. Fiz. **12**, 932 (1986) [Sov. Tech. Phys. Lett. **12**, 386 (1986)].
[54] H. Frahm and H. J. Mikeska, Z. Phys. B **60**, 117 (1985).
[55] F. Haake, M. Kus, and R. Sharf, *ibid.* **65**, 381 (1987).
[56] L. L. Buishvili and A. I. Ugulava, Fiz. Tverd. Tela (Leningrad) **25**, 2370 (1983) [Sov. Phys. Solid State **25**, 1361 (1983)].
[57] V. I. Kesaev and A. I. Ugulava, *ibid.* **27**, 1259 (1985) [Sov. Phys. Solid State **27**, 763 (1985)].
[58] K. N. Alekseev, G. P. Berman, and V. I. Tsifrinovich, Zh. Eksp. Teor. Fiz. **97**, 1277 (1990) [Sov. Phys. JETP **70**, 718 (1990)].
[59] A. I. Ugulava, Izv. Vyssh. Uchebn. Zaved. Ser. Radiofizika **30**, 748 (1987). [Radiofiz, Quantum Electron. **30**, 558 (1987)].
[60] E. A. Turov, M. I. Kurkin, and V. V. Nikolaev, Zh. Eksp. Teor. Fiz. **64**, 283 (1973) [Sov. Phys. JETP **37**, 147 (1973)].
[61] V. A. Ignatchenko and V. I. Tsifrinovich, Usp. Fiz. Nauk **133**, 75 (1981) [Sov. Phys. Usp. **24**, 42 (1981)].
[62] A. S. Borovik-Romanov, Yu. M. Bun'kov, B. S. Dumesh, et al., Usp. Fiz. Nauk **142**, 537 (1984) [Sov. Phys. Usp. **27**, 235 1984)].
[63] S. De Filippo, M. Fusco Girard, and M. Salerno, Physica D **29**, 421 (1988).
[64] E. A. Turov and M. I. Kurkin, *Problems of Magnetic Resonance* (in Russian), Nauka, M., 1978, p. 271.
[65] G. Müller, Phys. Rev. A **34**, 3345 (1986).
[66] G. M. Zaslavsky, Phys. Rep. **80**, 157 (1981).
[67] P. V. Elyutin, Usp. Fiz. Nauk **155**, 397 (1988) [Sov. Phys. Usp. **31**, 597 (1988)].
[68] M. V. Berry, Proc. R. Soc. London A **413**, 183 (1987).
[69] G. Casati, B. V. Chirikov, F. M. Izrailev, and J. Ford, *Stochastic Behavior in Classical and Quantum Hamiltonian Systems*, eds. G. Casati and J. Ford, Springer-Verlag, Berlin, 1979, p. 334.
[70] G. P. Berman and G. M. Zaslavsky, Physica A **91**, 450 (1978).
[71] T. Dittrich and R. Graham, Ann. Phys. (NY) **200**, 363 (1990).
[72] M. Feingold, N. Moiseyev, and A. Peres, Phys. Rev. A **30**, 509 (1984); M. Feingold and A. Peres, *ibid.* **31**, 3472 (1985).
[73] K. Nakamura, Y. Okazaki, and A. R. Bishop, Phys. Lett. A **117**, 459 (1986).
[74] K. Nakamura, Y. Okazaki, and A. R. Bishop, Phys. Rev. Lett. **57**, 5 (1986).
[75] H. Frahm and H. J. Mikeska, Z. Phys. B **65**, 249 (1985).
[76] F. Haake and D. L. Shepelyansky, Europhys. Lett. **5**, 671 (1988).
[77] M. Kus, J. Motowski, and F. Haake, Preprint Univ. Essen, FRG, 1988.
[78] M. Kus, R. Sharf, and F. Haake, Z. Phys. B **66**, 129 (1987).
[79] R. Sharf, B. Dietz, M. Kus, F. Haake, and M. V. Berry, Europhys. Lett. **5**, 383 (1988).
[80] S. Fishman, D. R. Grempel, and R. E. Prange, Phys. Rev. Lett. **49**, 509 (1982).
[81] J. E. Beyfield and D. Sokol, Phys. Rev. Lett. **61**, 2007 (1988); E. J. Galvez, B. E. Sauer *et al.*, *ibid.*, p. 2011.
[82] Ya. B. Zel'dovich, Usp. Fiz. Nauk **110**, 139 (1973) [Sov. Phys. Usp. **16**, 427 (1973)].
[83] I. C. Percival, J. Phys. B **6**, L229 (1973).
[84] D. Umberger and J. D. Farmer, Phys. Rev. Lett. **55**, 661 (1985); C. Grebogi, S. W. McDonald *et al.*, Phys. Lett. A **110**, 1 (1985).
[85] T. A. Brody, J. Flores, J. B. French *et al.*, Rev. Mod. Phys. **53**, 385 (1981).
[86] R. Grobe and F. Haake, Phys. Rev. Lett. **62**, 2893 (1989).
[87] V. S. Rukhlov, Pis'ma Zh. Eksp. Teor. Fiz. **52**, 1060 (1990) [JETP Lett. **52**, 454 (1990)]; V. V. Zverev, Abstracts of reports at the 20th All-Union Seminar "Spin Waves". L., 1990.

Translated by M. V. King